Table 3.7. Summary of Analysis Results (PRF = 20 MHz)

Operational Scenario Description					UWB Signal Characteristics							
GPS Application	UWB Single	UWB Multiple	UWB Indoor	UWB Outdoor	PRF (MHz)	Gating %	Mod.	GPS Receiver Architecture	Classification of Interfering Signal	Maximum Interference Threshold[1]	Maximum Allowable EIRP[2]	Comparison with the Current Part 15 Level (dB)
Terrestrial	X			X	20	20	OOK	C/A-code	CW-Like	-146.3	-106.9	35.6
Terrestrial	X			X	20	20	50% Abs.	C/A-code	Pulse-Like	-135	-95.6	24.3
Terrestrial	X			X	20	100	50% Abs.	C/A-code	Noise-Like	-138	-98.6	27.3
Terrestrial		X	X		20	20	OOK	C/A-code	CW-Like	-146.3	-91.3	20
Terrestrial		X	X		20	100	50% Abs.	C/A-code	Noise-Like	-138	-89	17.7
Terrestrial		X		X	20	20	OOK	C/A-code	CW-Like	-146.3	-96	24.7
Terrestrial		X		X	20	100	50% Abs.	C/A-code	Noise-Like	-138	-93.7	22.4
Maritime		X	X		20	20	OOK	C/A-code	CW-Like	-145	-75.4	4.1
Maritime		X	X		5	100	50% Abs.	C/A-code	Noise-Like	-138	-73.1	1.8
Maritime		X		X	20	20	OOK	C/A-code	CW-Like	-145	-81.8	10.5
Maritime		X		X	20	100	50% Abs.	C/A-code	Noise-Like	-138	-79.5	8.2
Railway		X	X		20	20	OOK	C/A-code	CW-Like	-145	-90	18.7
Railway		X	X		20	100	50% Abs.	C/A-code	Noise-Like	-138	-86.5	15.2
Railway		X		X	20	20	OOK	C/A-code	CW-Like	-145	-91.5	20.2
Railway		X		X	20	100	50% Abs.	C/A-code	Noise-Like	-138	-88.0	16.7
Surveying	X			X	20	100	50% Abs. & 2% Rel	Semi-Codeless	Noise-Like	-149.5	-92.6	21.3
Surveying		X		X	20	100	50% Abs. & 2% Rel.	Semi-Codeless	Noise-Like	-149.5	-92.7	21.4
Aviation-NPA		X		X	20	20	OOK	C/A-code	CW-Like	-145	-86.6	15.3
Aviation-NPA		X		X	20	100	50% Abs.	C/A-code	Noise-Like	-138	-84.3	13
Aviation-ER		X	X		Note 2	Note 2	Note 2	C/A-code	Noise-Like	-134.8	-76.6[3]	5.3
Aviation-ER		X		X	Note 2	Note 2	Note 2	C/A-code	Noise-Like	-134.8	-85.6[3]	14.3

Notes: En-Route Navigation (ER), Non-Precision Approach (NPA)

1. When the interference effect has been classified as pulse-like or noise-like, the value is expressed in units of dBW/MHz. The value is expressed in units of dBW when the interference effect has been classified as CW-like.
2. In this operational scenario, it is assumed that there is a large enough number of UWB devices, such that independent of the individual UWB signal parameters the aggregate effect causes noise-like interference.
3. This maximum allowable EIRP is based on an assumed density of 200 UWB devices per square kilometer transmitting simultaneously.

RTCA notes that as indicated in section 3.4.3.1, the interference effects upon the GPS receivers were classified as pulse-like, noise-like and CW like transmissions. The classification of a given UWB device is determined by the PRF, gating, and the modulation discipline. The modulation disciplines used in the NTIA program were no modulation, constant PRF with random on-off keying, or random dithering. The shape of the transmitted pulse determines the RFI spectrum. In practical UWB applications the spectrum is primarily determined by the pulse width which typically has width ≅ 0.5 to 1 ns. The data collection and analysis portion of the NTIA test program summarized the results in a three dimensional matrix where each point in the matrix is the measured receiver susceptibility level for that group of transmission parameters. The dimensions of this matrix were intended to cover the range of pulse-like, noise-like and CW like RFI transmissions.

Appendix B gives equations that allows the measured receiver susceptibility level to be estimated between the data points of the NTIA three dimensional measurement matrix. Three of the four cases treated in the appendix cover the transmission classifications measured in the NTIA test program. Case I in Appendix B represents CW-like transmissions, Case II represents noise-like transmissions, and Case IV represents pulse-like transmissions.

As an example extension of the measurement results, consider the Case II noise-like transmissions for C/A code receivers with UWB parameters 100% gating, 50% dither and 5 MHz PRF. The measured receiver susceptibility level for the reacquisition point under these conditions was -94 dBm/20MHz (Table 2.1 of NTIA special publication 01-45) . The corresponding interference threshold is -137dBW/MHz when the 20MHz measurement bandwidth was reduced to 1 MHz (-13dB) and the conversion from dBm to dBW (30dB) was made. This case is given for the non-precision scenario in Table 3.6 (third line from the bottom). Assume one wants the interference threshold when the PRF = 15MHz. Using equation (2) from Appendix B, and letting $\bar{R}_P = \bar{R}_5 = 5\text{MHz}$ and $B_h = 1\text{MHz}$, we have

$$P_{RFI} = \Phi(f_0)B_h\bar{R}_5 = -137\text{dBW in 1MHz bandwidth} \qquad (1)$$

Solving (1) for the energy spectral density per pulse, we have $\Phi(f_0)$ = -264 joules/Hz per pulse. For 1 ns pulse width, Φ is constant over ± 10MHz about f_0. For $\bar{R}_P = \bar{R}_{15} = 15\text{MHz}$, the interference power is

$$P_{RFI} = \Phi(f_0)B_h\bar{R}_{15} = -132.2\text{ dBW in 1MHz bandwidth} \qquad (2)$$

Since the reacquisition point remains the same, the energy per pulse must be reduced by 4.77dB so that P_{RFI} = -137 dBW/MHz or energy spectral density must be reduced to $\Phi(f_0)$ = -259.2 joules/Hz per pulse. This result is confirmed in Table 3.6 third line from the bottom where the non-precision scenario RFI has PRF = 20MHz and the interference threshold = -138 dBW/MHz which corresponds to the -137 dBW/MHz for 5MHz. Note that (1) in Appendix B becomes more accurate as the average PRF relative to B_h is increased.

4.0 RFI ENCOUNTER SCENARIO DEVELOPMENT

An RFI encounter scenario is defined by knowledge of the victim receiver, the propagation path and the RFI source. Key aspects of the receiver are its necessary performance characteristics in the presence of interference (RFI susceptibility) and the receiver antenna gain. The main characteristics of the propagation path are the source-receiver separation distance (constant or time-varying) and the type of propagation. The main RFI source characteristics are its emission parameters (power, modulation, etc.) and its antenna gain. RFI scenario development involves determination of these several parameters. With the parameter values, analysis using a radio interference link budget is possible. One form of RFI link budget analysis involves computing the product (i.e.; the logarithmic sum) of the RFI source power, the propagation loss (determined by separation distance and propagation type) and the receiver antenna gain in the direction of the RFI. The result is the incident interference at the victim receiver.

For aviation and maritime applications government regulatory agencies establish RFI protection limits for receivers against which they compare the offending interference. If the interference is less than the protection limit then the RFI is compatible for that scenario. If on the other hand, the RFI is greater than the protection limit, it is not compatible. Radio regulations establish the emissions requirements for transmitters or unintentional emitters to manage interference at the source.

Table 4.1 contains the link budget template to be applied to UWB RFI for the protection of GPS when used for safety of life service.

Table 4.1 GPS RFI Link Budget Template

1	Receiver Susceptibility Mask (for broadband noise)	Standard based on broadband noise receiver performance characteristics (RTCA DO 235)
2	Aeronautical or Public Safety Margin	Protects against unknown errors in link budget estimates
3	Total Allowed Broadband RFI (at receiver input)	Subtract logarithms 2) from 1)
4	Broadband Noise Equivalent Correction Factor	Determined using standardized test/analysis procedures (e.g. Stanford test or NTIA BWCF)
5	Multiple System Allotment (excluding MSS)	Used for composite of all UWB and all future RFI sources
6	Single Emitter Allotment	Allotment for each individual emitter of each system which makes up the composite.
7	RFI level at Victim Receiver	Add logarithms of 3), 4), 5), and 6)
8	Antenna Gain in Direction of RFI	Determined by operational scenario
9	Maximum RFI Propagation Loss	Based on separation distance determined by operational scenario (positive value)
10	Source RFI Emission Limit	RFI Emission Limit =(7) – (8) + (9) logarithms

As described above, Aeronautical Margin is an estimate of unknown errors that may exist in the RFI link budget. This margin is not available to non-aeronautical RFI sources. The intent of the multiple system and single emitter allotments is to recognize the current situation with the

existing out-of-band emissions from MSS mobile terminals and accommodate UWB and future RFI sources.

Note that the structure of Table 4.1 implies a linear model. This is so because the intensity of the RFI is typically maintained at a low level (< -160 dBW/MHz). Nonlinear effects such as might be caused by the UWB spike-like waveforms are not a consideration.

4.1. Aviation Approach Scenarios

For the approach scenarios considered thus far in this study, the principal interference is thought to be from mobile terrestrial sources. Future work, especially for the GPS L5 frequency, will treat other cases such as fixed terrestrial sources (DME ground transponders) and on-board aircraft equipment. To the extent that material becomes available, on-board passenger electronic interference sources may be studied as well.

RFI link budget analysis based on the interference mask requirements show that the loss of continuity would occur with unacceptable probability when the interfering power exceeds the receiver susceptibility mask. Loss of continuity due to RFI may occur in the vicinity of the precision approach decision height if the aircraft flight path deviations decrease the distance between the aircraft and the RFI source below the minimum separation distance. The aircraft total system error (TSE) is defined as the aircraft's deviation from its nominal decent path (e.g., 3° glideslope). The TSE probability distribution can be determined by convolving the flight technical error (FTE) distribution and the navigation system error (NSE) distribution as described Appendix D.

The risk of loss of continuity due to failures of the GPS signal-in-space is about one in 3.5 million approaches ($\sim 5\sigma$) over a 15-second exposure interval. The risk of continuity due to an RFI event is not strictly defined anywhere in the requirements. It is obviously important to keep this risk very low as loss of continuity may result in a go-around which is potentially disruptive to air traffic management and costly to airplane operators. Because the RFI continuity risk is influenced by factors that are not strictly part of the signal in space (i.e. the airplane FTE) it is inappropriate to apply the signal-in-space continuity requirement to this continuity risk. More will be said about a reasonable level of continuity risk for this potential source in Appendix D.

RF-induced loss-of-continuity events are a statistical problem. If the separation distance falls below the minimum, it is assumed that the RFI at the receiver exceeds its susceptibility limit and that with probability 1 that there will be a cycle slip in a 10 second interval. Therefore it is important to determine the probability that an aircraft on a Category II approach can get closer than the minimum separation distance to an interference source. It is assumed that an emitting RFI source can be anywhere within the obstacle clearance surface.

4.1.1 Minimum RFI Separation Distance and Link Budget for Category II/III Approaches

4.1.1.1 Category II/III Minimum Separation Distance:

The geometry between the interference source and an airplane on a Category II approach is illustrated in Figure 4.1. For the scenario it is assumed that there is one MSS mobile earth terminal and a collection of other mobile RFI sources such as UWB transmitters operating in the vicinity of the ground point under the Category II decision point. When airplane is at the 100 foot decision height point, it is assumed the RFI source(s) can be at the extreme of the obstacle clearance surface that is 15.1 feet above the ground. Hence the nominal 3° path is 100-15.1=84.9 ft above the RFI source. The GPS antenna is assumed to be top to the airplane so an additional 7 feet of altitude is included. If the airplane is to maintain a minimum separation of 70 ft, then the maximum allowable TSE is:

TSE = 84.9+7-70 = **21.9 ft.**

Further analysis (Appendix D) shows this is a reasonable distance with appropriate statistical significance.

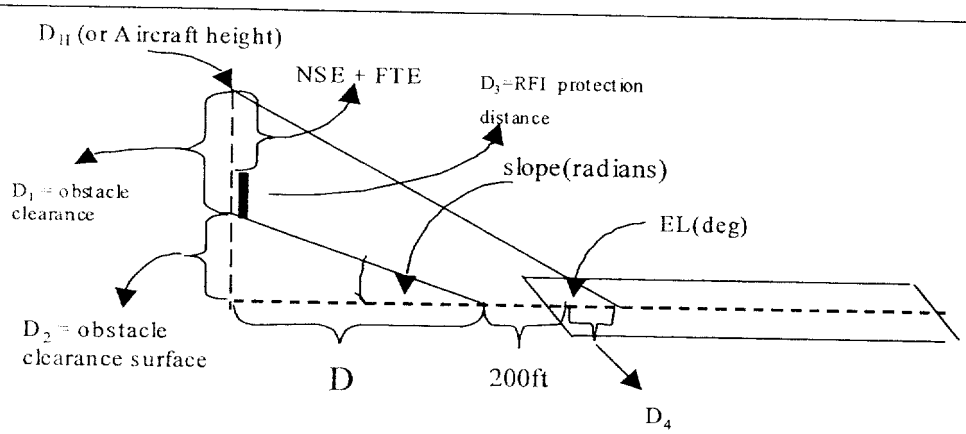

Aircraft antenna height above control point = 7ft

EL = 3 deg

D_H = 100 ft CAT II

D_4 = 50/tan(EL) ft

D = D_H/tan(EL) - D_4 - 200 = 754.1 ft for CAT II

slope = 1/50 for CAT II/III

D_2 = D*slope = 15.1 ft

Obstacle Clearance = D_1 = D_H - D_2 = 84.9 ft

aircraft antenna-to-obstacle surface = 84.9 + 7 = 91.9 ft

Figure 4.1 Category II/III Approach Geometry

The Category III vertical encounter geometry is the same as Category II up to the Category II decision point. Calculations for a lateral RFI encounter geometry suggest that lateral RFI on taxiway at threshold has a separation distance of 184ft which results in a 76.4 dB path loss given a –5dbi antenna gain. Comparison with the link values in Table 4.2 shows that the Category II vertical encounter is the more stringent case.

4.1.1.2 Precision Approach RFI Link Budgets:

Table 4.2 lists the parameters of the Category II/III scenario developed by SC-159 as described above. Previously developed Category I scenario values are adapted to the new situation of multiple mobile UWB and other RFI sources by same method.

Table 4.2. GPS Precision Approach RFI Link Budgets

	GPS WAAS/LAAS Category I	**GPS LAAS Category II/III**
Frequency	1575 MHz	1575 MHz
Receiver Susceptibility Mask (broadband noise)	-140.5 dBW/MHz	-140.5 dBW/MHz
Aeronautical Margin	-5.6 dB	-5.6 dB
Total Allowed Broadband RFI (at receiver input)	-146.1 dBW/MHz	-146.1 dBW/MHz
Worst-Case UWB Noise Equivalent Correction Factor (note 1)	-10 dB	-10 dB
Multiple System Allotment (excluding MSS)	-10 dB	-10 dB
Single Emitter Allotment (note 2)	-10 dB (strawman value until data available)	-10dB (strawman value until data available)
UWB RFI @GPS receiver	-174.1 dBW/MHz	-174.1dBW/MHz
Antenna gain toward RFI source	10 dB	13.1dB
Propagation Loss (separation distance)	66.1 dB (100ft)	63.0 dB (70ft)
RFI Emission Limit	-100 dBW/MHz	- 100 dBW/MHz

Notes: 1) Testing to date has shown that some UWB test waveforms can produce interference that is 10 dB worse than broadband noise. While this worst case must be accounted for, current data shows that the correction factor is highly modulation specific. Some test modulations (high dithering, low duty cycle) may result in a less negative correction factor. See section 3.1.

2) Discussion in Appendix C shows the need for a factor to handle the aggregate (cumulative) effect of RFI from multiple mobile sources such as UWB sources. The value of that factor should allow for at least the density of vehicle-mounted interference sources on a heavily traveled roadway. That value should be at least 10 dB (i.e.; the effect of 10 UWB units transmitting non-concurrently, with power combining linearly).

There have been several significant interference issues that necessitated the development of international standards. Examples include ILS (FM-broadcast RFI), MLS (MSS FLES RFI), and

GPS (MSS MET RFI). These aviation safety-of-life systems had to accommodate the indicated RFI. With the exception of GPS, each aeronautical navigation system adopted the informal frequency management procedure that the RFI must be 8[32] to 12 dB below the victim receiver's noise floor. This RFI practice is common in the national civil aviation agencies of ICAO and the industry /government committees of RTCA and EUROCAE. The procedure is invoked whenever a safety-of-life system does not have margin in its link budget to absorb RFI. This is the case for GPS since the MSS mobile terminal received essentially all of Total Allowed RFI. Therefore the Multiple System Allotment to additional system must be small. The chosen value, consistent with past practice, is –10 dB. The worst-case noise equivalency factor value (–10 dB) is based at present on the known ratio of the receiver susceptibility for CW RFI to that for broadband noise power in a 1 MHz bandwidth.

Compared to Category I, Category II operations must makeup a potential 3 dB deficit in link margin from to smaller 70 ft. by reducing the antenna gain toward the RFI from –10 dB to -13.1dB. This reduction is justified because of the sizes and types of aircraft certified for Category II have lower installed GPS antenna gain in the lower hemisphere. Note also that the required UWB RFI emission level (–100 dBW/MHz) is 28.7 dB below the proposed Part 15 limit of –71.3 dBW/MHz

4.1.2 Non-precision Approaches

Regulatory agencies define enroute airways and terminal area approach paths by a series of waypoints connected by straight-line segments. Each waypoint is assigned a name and a location such as initial approach point, final approach point and missed approach point. About each waypoint is a rectangular protected displacement area. For the TSO-129 GPS the dimensions of the displacement area at the missed approach point are ± 0.5 nautical miles by ± 0.3 nautical miles; its center is at the runway threshold for straight-in approaches (Figure 4.1). By contrast Category I precision approaches have an "effective" lateral displacement of ± 350ft (full-scale deviation of the ADI display) at the runway threshold.

The FAA distinguishes a precision approach from a non-precision approach by requiring a precision approach to have combined lateral and vertical (glide slope) guidance. The term non-precision approach refers to facilities without the vertical guidance of a glide slope. This however does not imply an unacceptable quality of guidance. The FAA maintains the same level of flight safety for non-precision approaches as it does for precision approaches. They achieve this by requiring a much larger protected displacement area at the missed approach point and a higher minimum descent altitude (MDA) for non-precision approaches than they do for the precision approach. The MDA is the lowest altitude to which descent shall be authorized prior to seeing the airport for procedures not using a glide slope. For precision approaches, the term used for this corresponding altitude is decision height (DH), the height above the runway threshold. Note: for ILS, the Category I DH is 200ft. During a non-precision approach, the pilot can manage his descent using any vertical profile he chooses subject to the constraints of his aircraft and navigation equipment. He may for example descend to the MDA and then fly a constant altitude flight path to the runway. He also must determine the time in advance that he will arrive

[32] Recommendation ITU-R IS.1009-1, "Compatibility between the Sound-Broadcasting Service in the band of about 87-108 MHz and the Aeronautical Services in the band 108-137 MHz.

at the missed approach point, which is usually prior to the runway threshold. If he cannot see the runway environment at that time he must perform a missed approach.

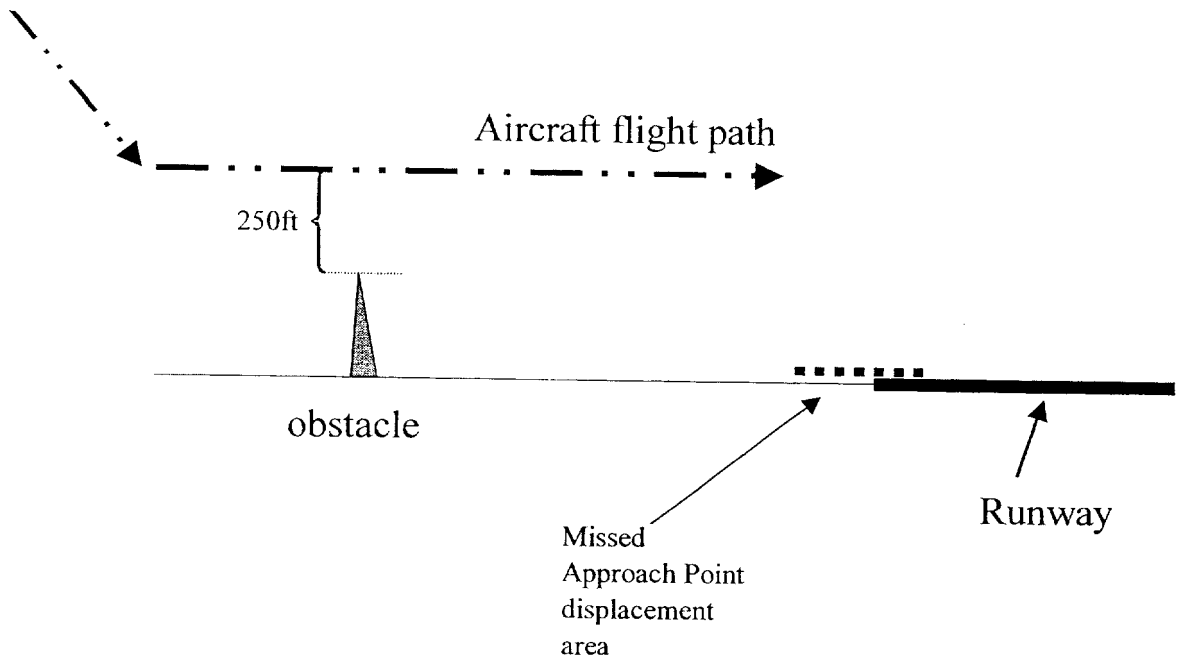

Figure 4.2 Non-Precision Approach Geometry

Associated with each non-precision final approach segment (Fig. 4.2) there is an MDA. In general, the MDA = 250 feet above the airport + (obstacle height). If there are no obstructions, then the MDA = 250 feet above ground. The RFI separation distance calculations will use the 250 foot value for two reasons. An RFI source can be on top of the obstacle or it can be an obstacle free zone and MDA = 250feet above the highest point. An additional 7 feet is added to account for the aircraft antenna displacement from the aircraft control point. Thus the calculation to determine the RFI separation distance is expressed as:

Separation distance = 257 ft – TSE (Eq 1);

where the total system error, TSE, is the root-sum-square of the flight technical error, FTE, and the navigation system error, NSE. The separation distance will be calculated corresponding to a 95 % probability. Table 1-1 of RTCA/DO-208 gives the vertical FTE = 100 ft (95%) while the vertical NSE for the vertical guidance component is given in Table 2-3 of RTCA/DO-208 as 68 ft (95%). This means that the 2 σ vertical position error is:

$$TSE = \sqrt{100^2 + 68^2} = 121\text{ft}.$$

Therefore from (Eq. 1) separation distance = 257 – 121 = 136ft.

4.2 Other Aviation Scenarios

4.2.1 Aircraft Surface Movement Scenario

Work on this scenario is incomplete as of the time of this second interim report. Further development is planned and the analysis is to be inserted in the RTCA final report.

4.2.2 Aircraft Enroute Navigation with On-board Personal Electronic Device RFI

Based on the proliferation of wireless products and services, including the potential of UWB devices operating in safety-of-life bands, the aviation industry is providing the following data relating to critical operational scenarios. The need for such data is based on the fact that numerous unlicensed intentional and unintentional radiating devices are appearing onboard commercial aircraft. Extensive studies have been done to quantify the likelihood that any of these devices may cause harmful interference to aircraft communications and navigation systems. For the purpose of identifying the risks to Global Navigation Satellite Systems, particularly GPS, there have been over 2,160 measurements made from numerous points within many aircraft to identify path losses between GPS antennas and radiators inside the passenger cabin.

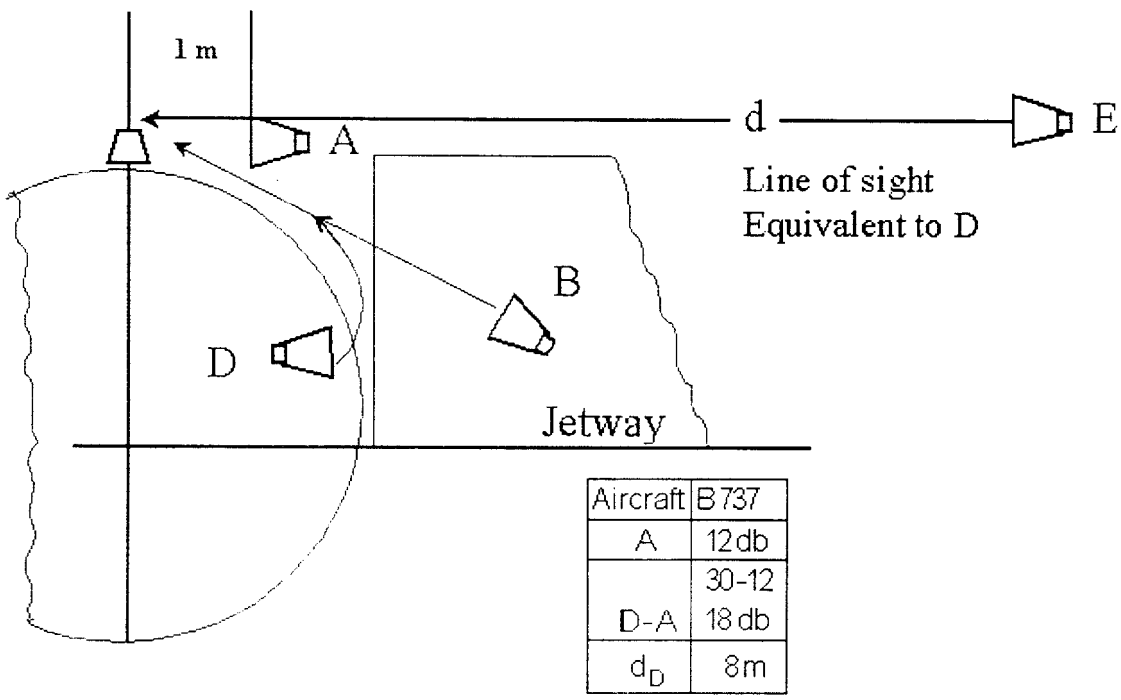

Figure 4.3 Aircraft Path Loss Determination

In Figure 4.3 above, the reference antenna placed at distance of one free space meter from the onboard GPS antenna yielded a total system path loss of 12 dB. Testing from within the aircraft yielded a worst case excessive path loss (D-A) of 18 dB. This represents a free space equivalent distance of 8 meters.

4.2.3 Aeronautical Mobile Satellite (Route) Service (AMS(R)S) Scenario Development and RFI Impact Assessment

The following text was supplied by RTCA Special Committee 165.

4.2.3.1. AMS(R)S Operational Scenario

The operational scenario is presently under development but will likely be similar to that for GPS enroute.

4.2.3.2. AMS(R)S Receiver Susceptibility and Interference Emission Limits

The interference criteria for AMS(R)S (Aeronautical SATCOM safety-of-life service) were established in RTCA DO-215 in terms based on system-level interference criteria as used in the ITU-R. The quantitative aspects of those criteria, slightly modified, were incorporated in ITU-R Recommendation M.1234, and were subsequently updated in RTCA DO-215A Change No. 1.

The AMS(R)S MASPS, scheduled for completion by July 2001, will repeat the DO-215A criteria. The specific criteria are predicated on observing the apparent increase of a "victim" system's noise floor temperature caused by interference and expressed as $\Delta T/T$. For single-entry interference (that due to any interfering system or "network"), $\Delta T/T$ shall be not greater than 6 %; and shall be not greater than 25 % for all sources of interference. "All sources" includes both inter- and intra-system interference.

RTCA DO-210D (MOPS for AMSS avionics) defines the minimum requirements for Aeronautical Earth Stations (AESs), including the maximum avionics system noise temperature and the consequent susceptibility of the AES receiver system based on the DO-215A Change No. 1 requirements. The maximum single-entry interference level is -163.2 dBm in the band 1529 - 1560 MHz, with increasing levels defined outside that band. It is noted that this level may impose more severe requirements on other interfering system than do some other aviation applications. SC-165 is currently investigating the specific effects of UWB-type interference.

Table 4.3. DO-210D AMSRS Receiver Susceptibility vs. Frequency

Frequency Range	Maximum Interference Level
470 to 1450 MHz	+3 dBm
1450 to 1529 MHz	Decreases linearly in decibels from +3 dBm at 1450 MHz to –72 dBm at 1529 MHz
1529 to 1560 MHz	-163.2 dBm
1560 to 1626.5 MHz	Increases linearly in decibels from –72 dBm at 1560 MHz to +3 dBm at 1626.5 MHz
1626.5 to 1660.5 MHz	+47.8 dBm
1660.5 to 18000 MHz	+3dBm

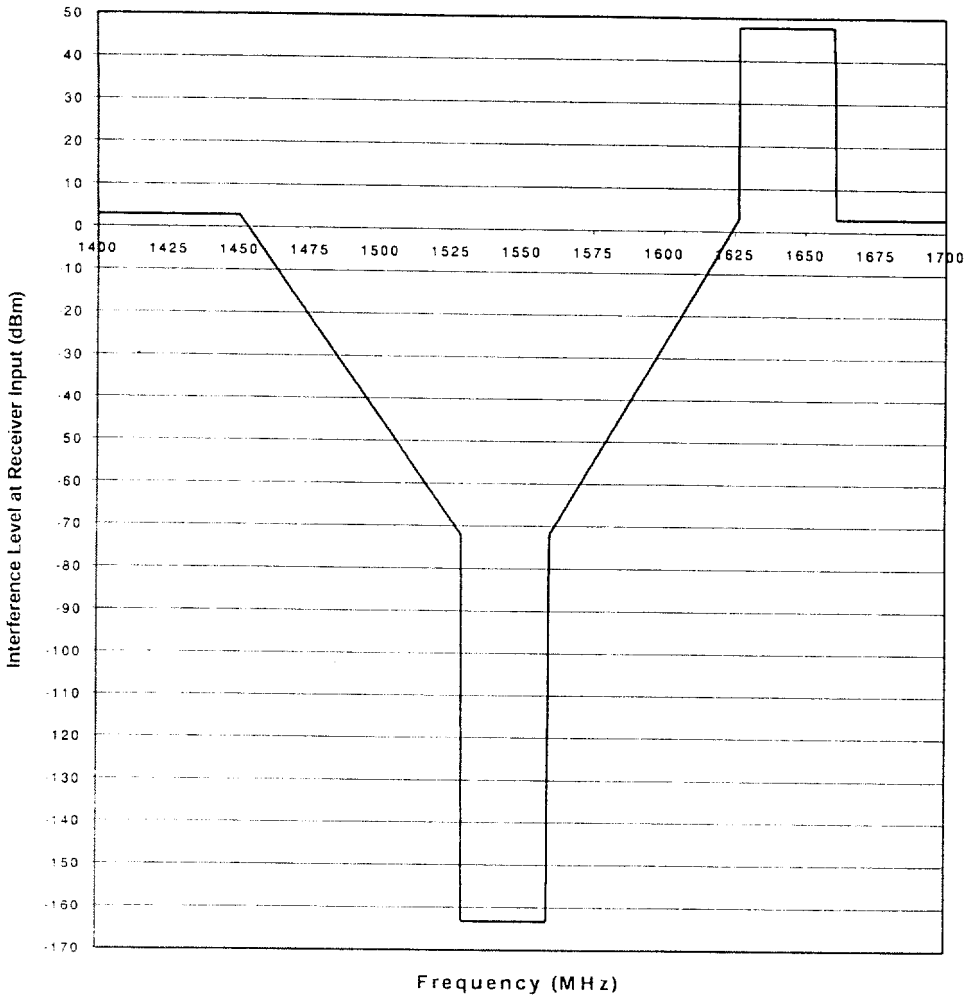

Figure 4.4. AMS(R)S Receiver Susceptibility for Single Entry Narrowband RFI

4.3 Non-Aviation Scenarios

When DOT tasked RTCA to study the GPS L5 and later the L1 interference environments, aviation-related issues were acknowledged to be of primary importance. The group was, however, encouraged to seek significant involvement and input from non-aviation GPS uses, especially public safety applications (e.g., maritime, E-911, police, fire fighting). The following section is the result of that input. More information is expected from maritime and other applications

4.3.1 Enhanced 911

The following material was presented to the RTCA study group at the most recent meeting.

4.3.1.1 E-911 Background

One very important Public Safety scenario is that of the Enhanced 911 (E911) Emergency Calling Systems. CC Docket No. 94-102, *Third Report and Order*, dated October 6, 1999, stated, "To improve public safety and extend ALI to wireless callers, the Federal Communications Commission has established a schedule, subject to certain conditions, for deployment of E911 features by wireless carriers." The following are excerpts from that Report and Order:

"In Phase I, which began on April 1, 1998, Public Safety Answering Points (PSAPs) were to receive a rough estimate of a caller's location and a dialable call-back number. In Phase II, scheduled for October 1, 2001, or six months after the service is requested, whichever is later, PSAPs are to receive a much more precise location identification, within 125 meters or about 410 feet of the caller's location."

"Wireless carriers who employ a Phase II location technology that requires new, modified or upgraded handsets (such as Global Positioning Systems (GPS)-based technologies) may phase-in deployment of Phase II subject to the following requirements:

Without respect to any PSAP request for Phase II deployment, the carrier shall:

1. Begin selling and activating ALI-capable handsets no later than March 1, 2001;
2. Ensure that at least 50 percent of all new handsets activated are ALI-capable no later than October 1, 2001; and
3. In addition to the 50 percent requirement, ensure that at least 95 percent of all new digital handsets activated are ALI-capable no later than October 1, 2002.

Once a PSAP request is received, the carrier shall, in the area served by the PSAP:

1. Within six months or by October 1, 2001, whichever is later:
   a. Ensure that 100 percent of all new handsets activated are ALI-capable;
   b. Implement any network upgrades or other steps necessary to locate handsets; and
   c. Begin delivering to the PSAP location information that satisfies Phase II requirements.

2. Within two years or by December 31, 2004, whichever is later, undertake reasonable efforts to achieve 100 percent penetration of ALI-capable handsets in its total subscriber base.

To be allowable under our rules, an ALI technology that requires new, modified, or upgraded handsets shall conform to general standards and be interoperable, allowing roaming among different carriers employing handset-based location technologies."

The FCC adopted the following revised standards for Phase II location accuracy and reliability: For handset-based solutions: 50 meters for 67 percent of calls, 150 meters for 95 percent of calls.

Later, in the 4th Memorandum Opinion and Order, dated September 8, 2000, the above schedules were modified as follows:

"We modify the rules for carriers employing handset-based ALI solutions in the following respects:

- Extend from March 1, 2001 to October 1, 2001, the date for carriers to begin selling and activating ALI-capable handsets.
- New Activations:
    - We eliminate the separate phase-in schedule that is triggered by a PSAP request.
    - We adopt the following revised phase-in schedule:
        - December 31, 2001: at least 25 percent of all new handsets activated are to be ALI-capable;
        - June 30, 2002: 50 percent of all new handsets activated are to be ALI-capable;
        - December 31, 2002 and thereafter: 100 percent of all new digital handsets activated are to be ALI-capable.
- Penetration:
    - Extend from December 31, 2004, to December 31, 2005, the date for carriers to reach full penetration of ALI-capable handsets in their total subscriber bases.
    - Modify the operational definition of full penetration from "reasonable efforts" to achieve 100 percent penetration of ALI-capable handsets to a requirement that 95 percent of all handsets in a carrier's total subscriber base be ALI-capable."

In that memorandum, some manufacturers raised questions on the feasibility of the schedule. Others, using GPS or a hybrid approach for the capability, agreed that it was feasible. Sprint stated "the only way to ensure compliance with the phase-in rule would be to sell only Global Positioning System (GPS) handsets effective October 1, 2001, which would limit consumer choice and potentially force consumers to pay high prices for first generation handsets." However, in the discussions part of the memorandum, it was pointed out by the Commission "At the time of the adoption of our current rules, substantial evidence existed establishing that ALI solutions had been tested successfully in field trials." Most of these solutions used GPS. Some were network-based CDMA solutions. The increased availability of GPS chips for the handset solution was also stated.

To meet the FCC mandate for E911 ALI services within schedule, GPS will be an integral part of the E911 services. This includes the use of GPS anywhere – inside of buildings, under trees, in

urban canyons. This is not to say that GPS will be the only sensor. Some of the proposed solutions are "hybrid" solutions that use both GPS and network-based CDMA measurements, but GPS is still an integral part of this safety-critical service.

4.3.1.2 E911 GPS Indoors

For the E911 handset application, GPS must be used indoors. That technology has been developed. QUALCOMM now owns the technology originally developed by SnapTrack, now owned by QUALCOMM. QUALCOMM developed an enhanced GPS sensor gps*One*™ to support E911 Phase II services using a handset-based technology mandated by the FCC. The technology takes advantage of the communication link between the wireless device and the infrastructure and has many modes of operation. In one mode of operation, the wireless device collects measurements from the GPS constellation and the terrestrial network and sends the information back to a location server in the network. The server also receives terrestrial measurements made by the base stations. The location server fuses the measurements together to produce an accurate position. Alternatively, the wireless device may compute the location itself instead of sending the measurements to a location server. Because of the enhanced sensitivity, gps*One*™ based sensors are able to work indoor and under severe shadowing conditions. This is an important life saving feature as far as E911 is concerned, and was developed in time to meet the FCC mandated schedules.

The specification for the GPS signal level under clear view of the sky is –130 dBm. Building penetration, shadowing, and foliage could degrade the signal by more than 20 dB. These weaker signals require more processing gain (longer integration) for successful acquisition. Knowing "true" GPS time at the wireless device and the approximate range to the satellite enables the wireless device to integrate the GPS signal coherently over much more than 20 milliseconds (one GPS navigation bit period. This is because the base station can predict the bit sequence for some parts of the navigation message, and the bit polarity can be sent to the wireless device to help with integrating coherently over multiple bits. QUALCOMM states that its bit prediction algorithm achieves an accuracy of about 99.5% and further states that gps*One*™ based GPS sensors are able to acquire and track GPS signals as weak as –150 dBm. Doppler and timing information used for signal acquisition are also established via CDMA communication with the base station. At such a low signal level however, even a small amount of interference can have adverse effects.

4.3.1.3 E911 GPS Outdoors

The E911 GPS scenario outdoors can be similar scenario as for indoors due to operation in urban canyons, under trees, etc. There can also be severe multipath fading because of structures, and the wireless device will be more susceptible to other interference.

4.3.1.4 E911 UWB Environment

The interference with the most serious potential for the indoor environment is that from UWB Wireless Local Area Networks (WLANs). These WLAN devices can be very close to an E911 user, and are expected to be very high PRF devices.

Since these types of WLANs can be collocated with E911 GPS devices, there is a potential for GPS reception degradation and more work is needed to further develop the scenario.

4.3.1.5 Summary and Conclusions

In conclusion, E-911 relies heavily on GPS for position reporting. Furthermore, indoor, urban canyon and foliage make certain GPS operations much more sensitive to interference. UWB Wireless Local Area Networks have already been announced, using very high PRFs and may be used widely. The Part 15 EIRP limit of –71.3 dBW/MHz results in a received level at 3 meter separation 24.3 dB above the GPS receiver noise floor. Unless UWB device EIRP values are reduced below that level, excessive interference to GPS-based E-911 operations may result. Further work is needed to quantify the scenario.

APPENDIX A GPS RECEIVER UWB RFI EFFECTS MODEL – BASIS FOR INTERFERENCE LINK BUDGET

This section provides some insight into how UWB affects GPS Receivers by looking into it with an analytical perspective. This insight validates the test results obtained by Stanford University. It also validates the use of the 10 dB correction factor that is the difference between the application of CW and noise interference.

A.1 UWB Pulse Characteristics

UWB implies the transmission of narrow pulses with fast rise times. If they were not narrow with fast rise times, they would not be UWB. How narrow and how fast defines the UWB spectrum. Figures A.1 and A.2 illustrate example UWB pulses – the first having a 1 ns pulse width, while the second has a 0.25 ns width.

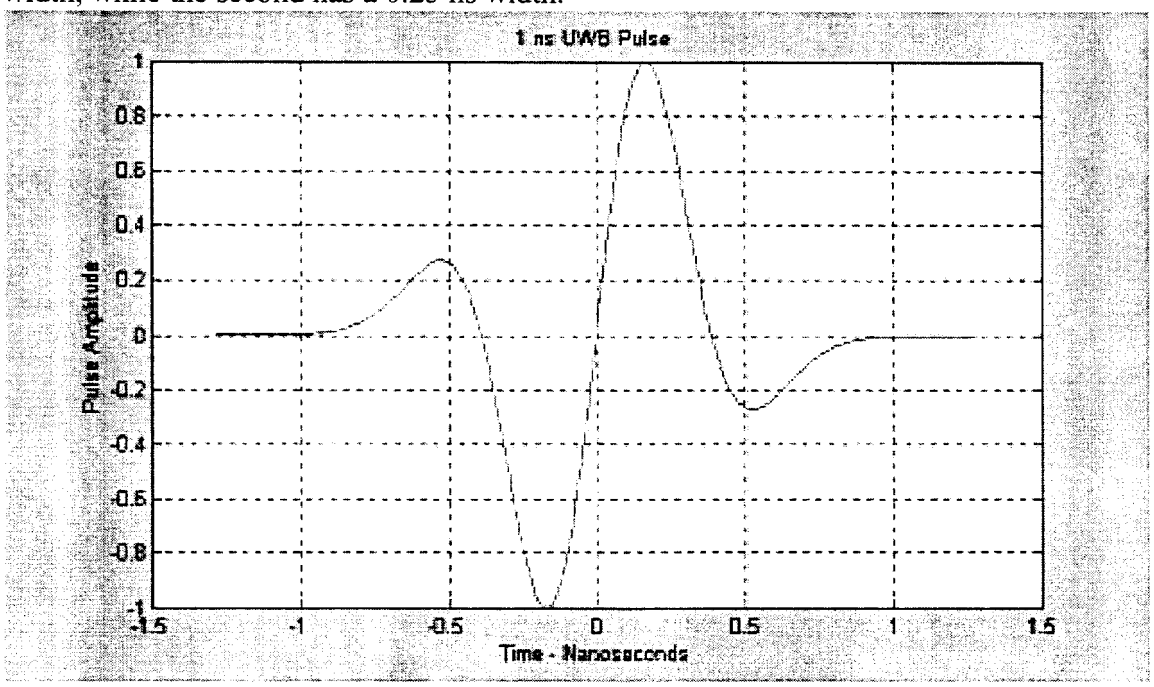

Figure A.1 One-Nanosecond UWB Pulse

The width of the pulse affects its spectral content significantly. For example, the spectral densities of the pulses shown in Figures A.1 and A.2 are shown in Figures A.3 and A.4. Note that the power spectral density (PSD) of the narrow pulse (Figure A.4) is centered at about 4.5 GHz, while the PSD of the wider pulse (Figure A.3) is centered at about 1.25 MHz, which is very close to the GPS band.

The difference between these two pulse-widths is significant, but so is the difference in their PSDs. This emphasizes that the any pulse stretching can significantly alter the PSD of a transmitted pulse that is intercepted by a GPS receiver. This pulse stretching could be caused by transmit-antenna non-linearities, transmission through walls or windows or collision with other pulses or multipath pulses.

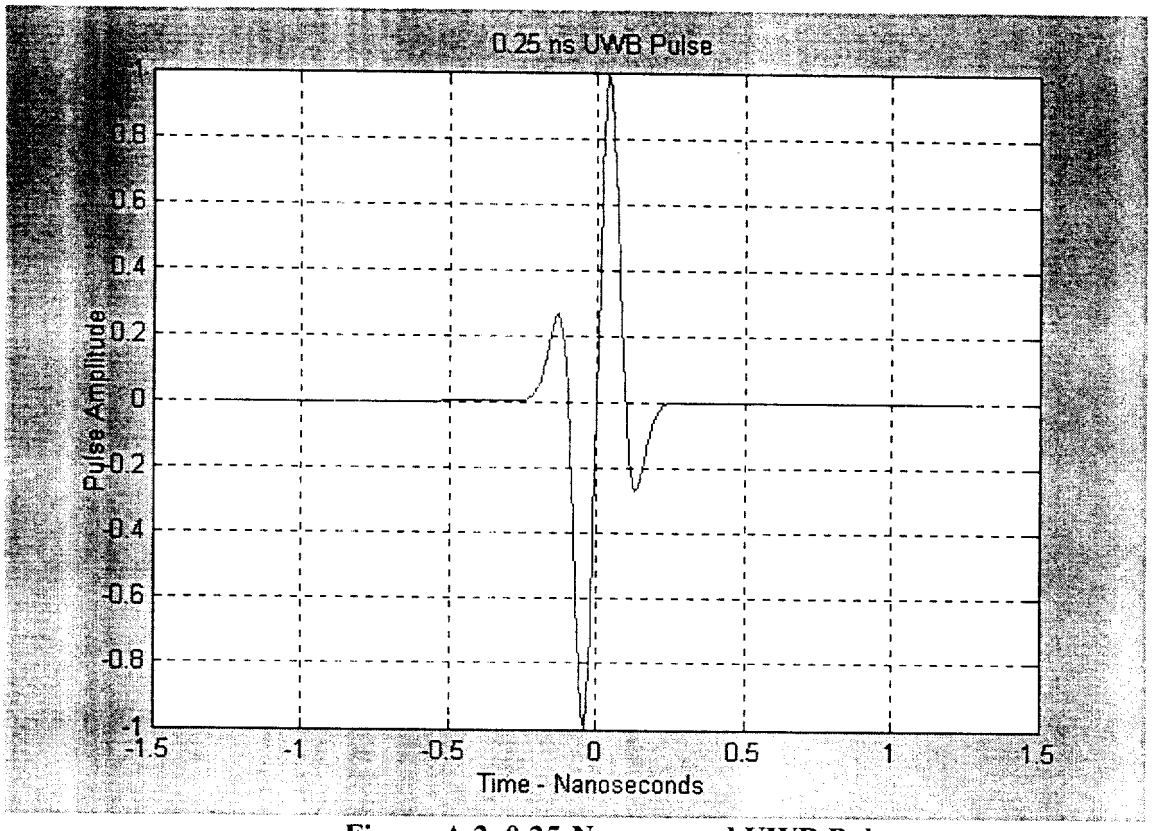

Figure A.2 0.25-Nanosecond UWB Pulse

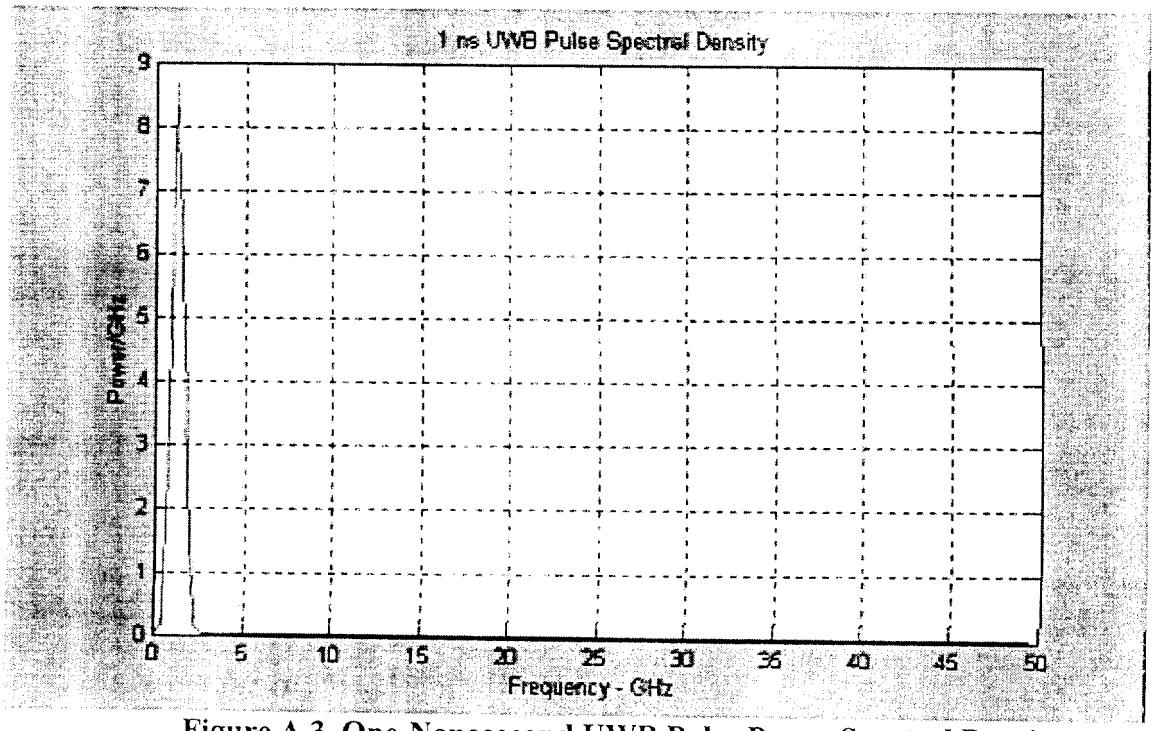

Figure A.3 One-Nanosecond UWB Pulse Power Spectral Density

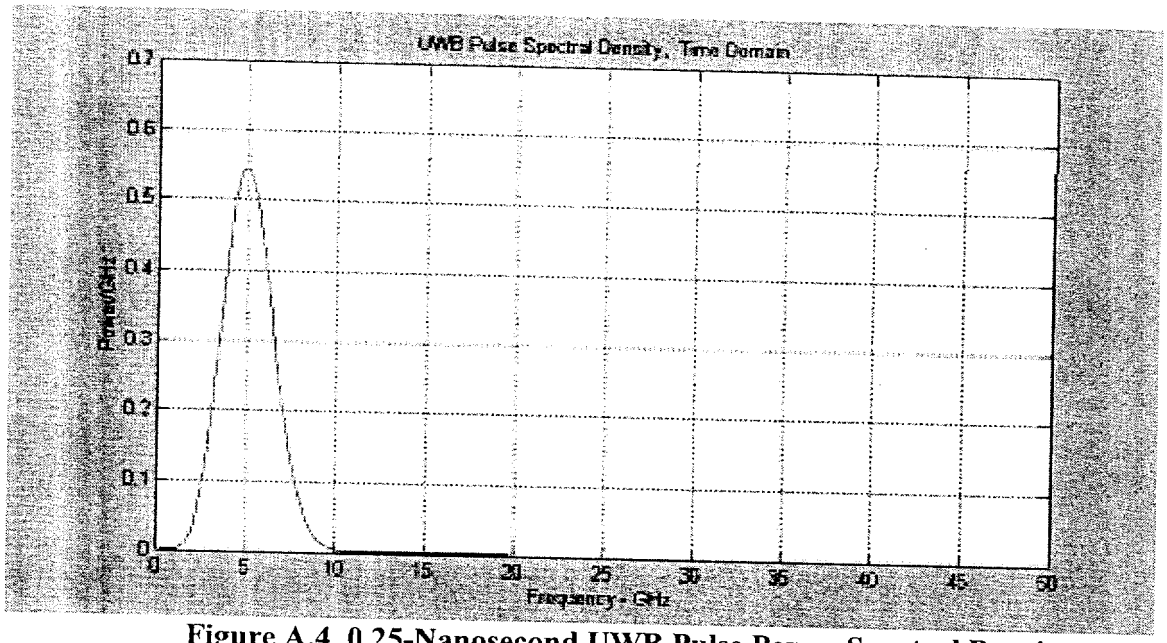

Figure A.4 0.25-Nanosecond UWB Pulse Power Spectral Density

A.2 Sequences of UWB Pulses

If one generates a sequence of UWB pulses, the PSDs change somewhat. Figure A.5 is a sequence of 6555 pulses occurring at uniformly random times with uniformly random amplitudes covering about 1311 microseconds. The pulses were added so that overlapping pulses were added together. This sequence simulates the reception of pulses from multiple sources at multiple distances, including pulses caused by multipath. The PSD for this sequence is shown in Figure A.6. Note that there is a slight shift compared to the single-pulse PSD of Figure A.4, probably caused by pulse collisions that can change the shape of the PSD. The probable reason for this is discussed below

Figure A.7 shows the PSD result of a similar sequence of one-nanosecond pulses. In this case, the reshaping of the PSD is somewhat more pronounced, probably because, with the wider pulse, the probability of pulse collision is higher.

Figure A.8 is a sequence of pulses at a constant PRF of 19.6875 MHz (1.575 GHz/80). Figure A.9 shows the PSD of this sequence, close-in near 1575 MHz. Note that there is a spectral line right at 1575 MHz.

A.2.1 What the GPS Receiver (Correlator) Sees

The pulse sequences described above were applied to a 20 MHz 6th-order Butterworth filter centered at 1575 MHz. A typical output of that filter for the random sequence of 0.25-nanosecond pulses is shown in Figure A.10. Very little can be discovered from that figure because of the presence of the 1575 MHz carrier. The effect of the filtering can be better observed at baseband. Thus, the filter output was mixed with a 1575 MHz carrier to convert the output to in-phase (I) and quadraphase (Q) components.

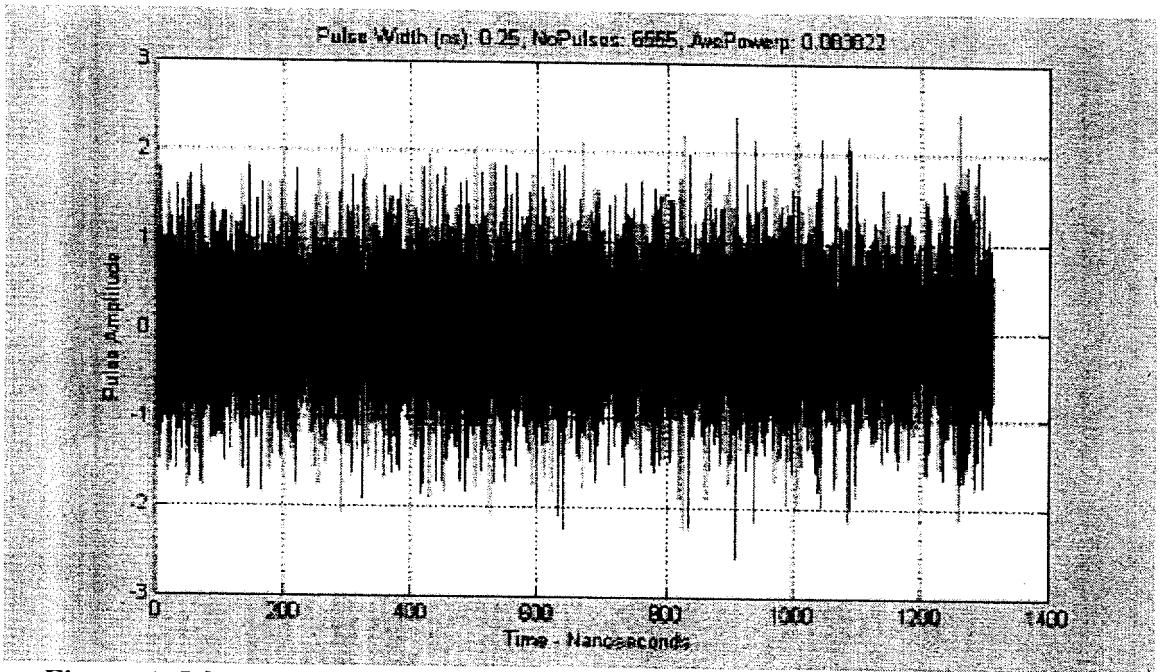

Figure A.5 Sequence of Uniformly Random Amplitude 0.25-Nanosecond UWB Pulses Occurring at Uniformly Random Times

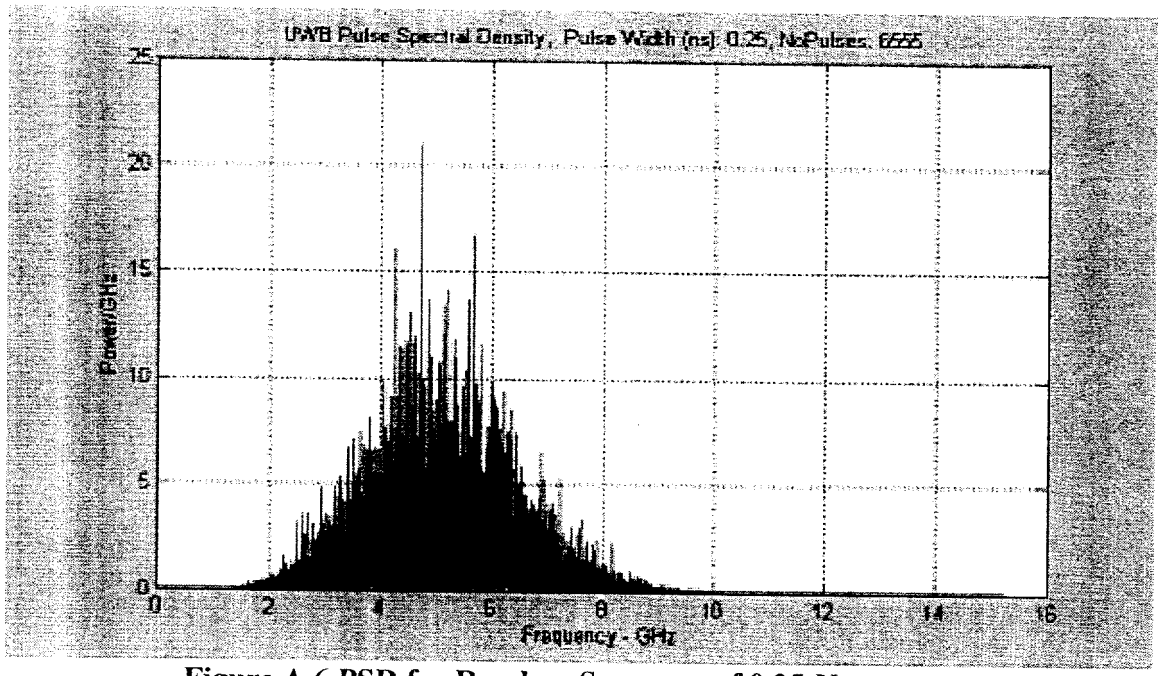

Figure A.6 PSD for Random Sequence of 0.25-Nanosecond Pulses

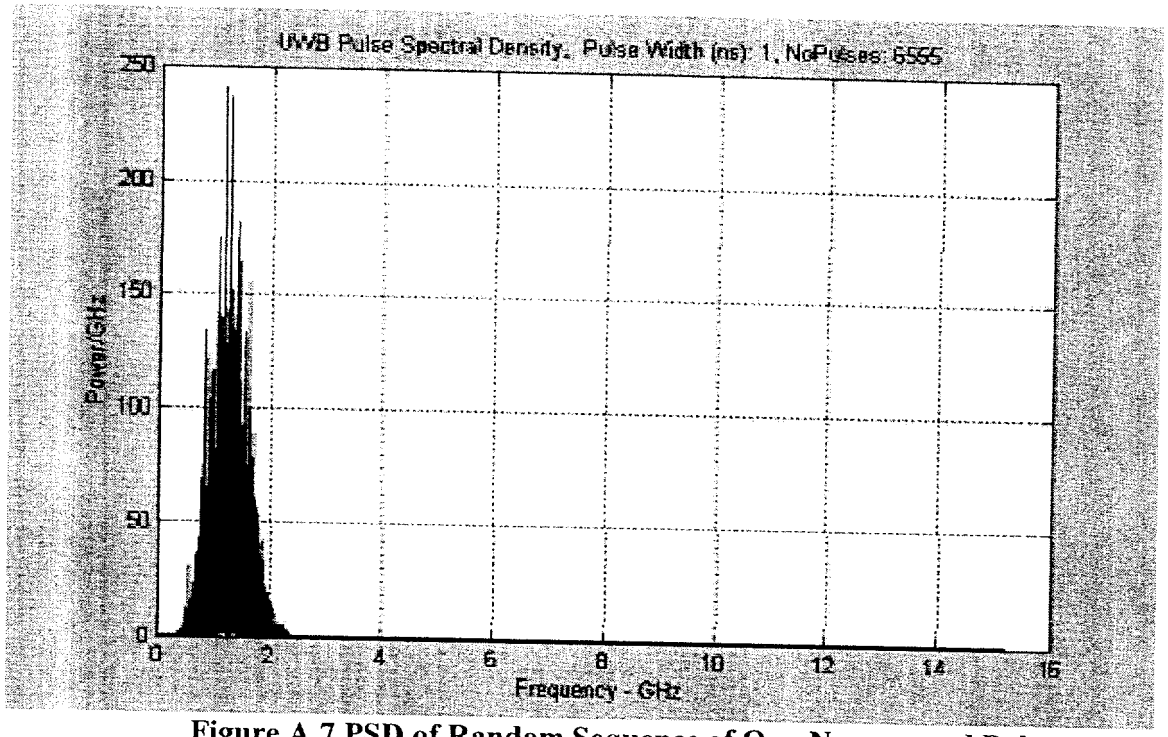

Figure A.7 PSD of Random Sequence of One-Nanosecond Pulses

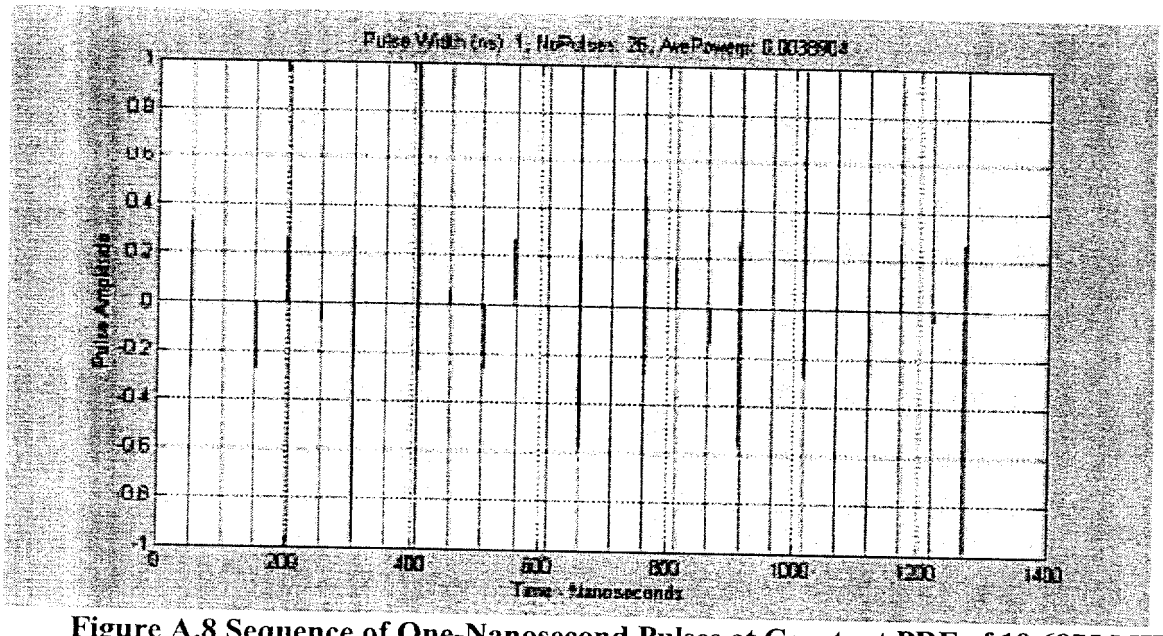

Figure A.8 Sequence of One-Nanosecond Pulses at Constant PRF of 19.6875 MHz

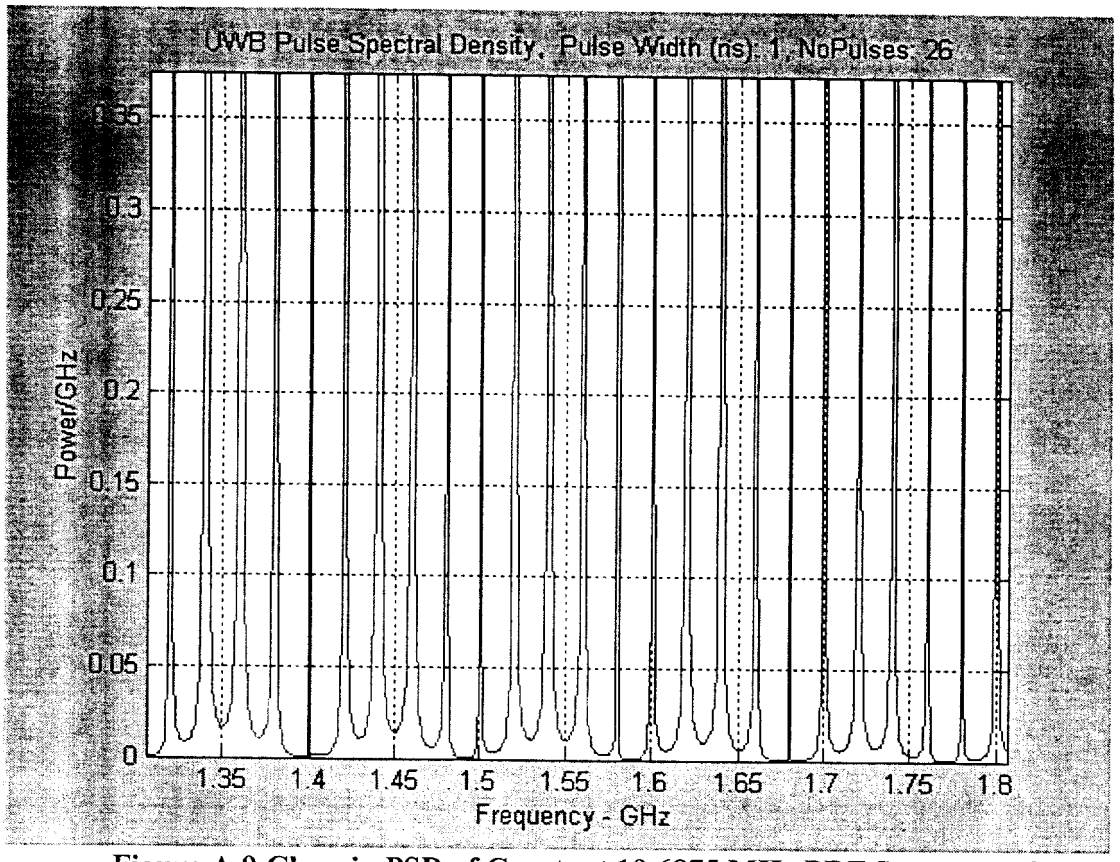

Figure A.9 Close-in PSD of Constant 19.6875 MHz PRF Sequence of Pulses

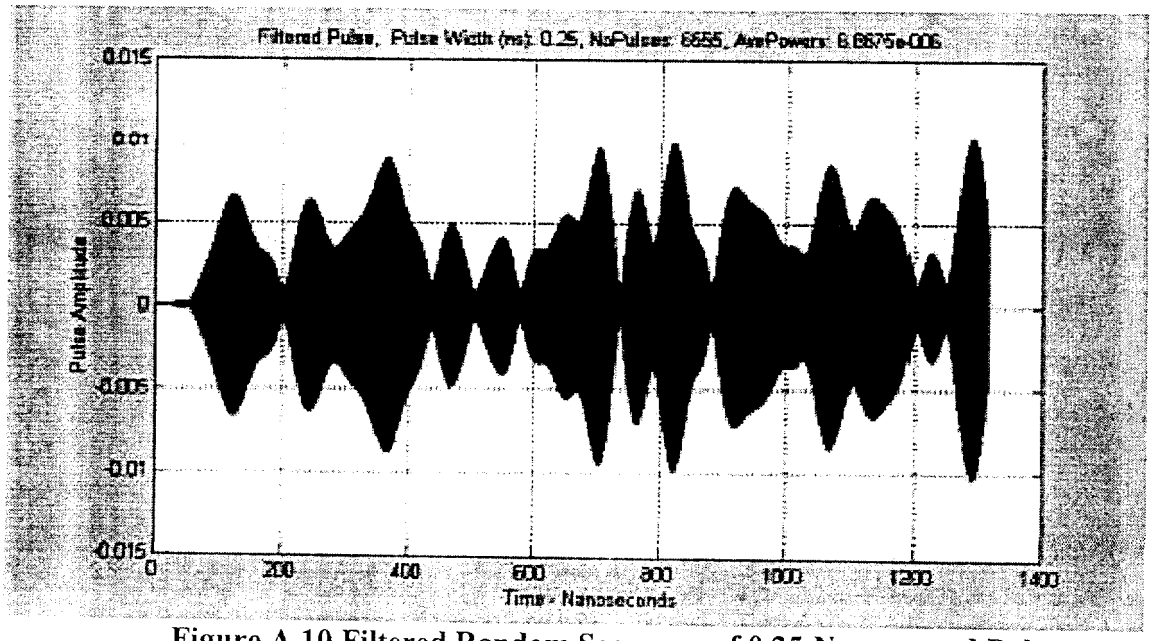

Figure A.10 Filtered Random Sequence of 0.25-Nanosecond Pulses

The I and Q components corresponding to the RF filter response shown in Figure A.10 are illustrated in Figures A.11 and A.12. Note that the average power was reduced by 37.84 dB, primarily because the pulse PSD was mostly above the GPS band.

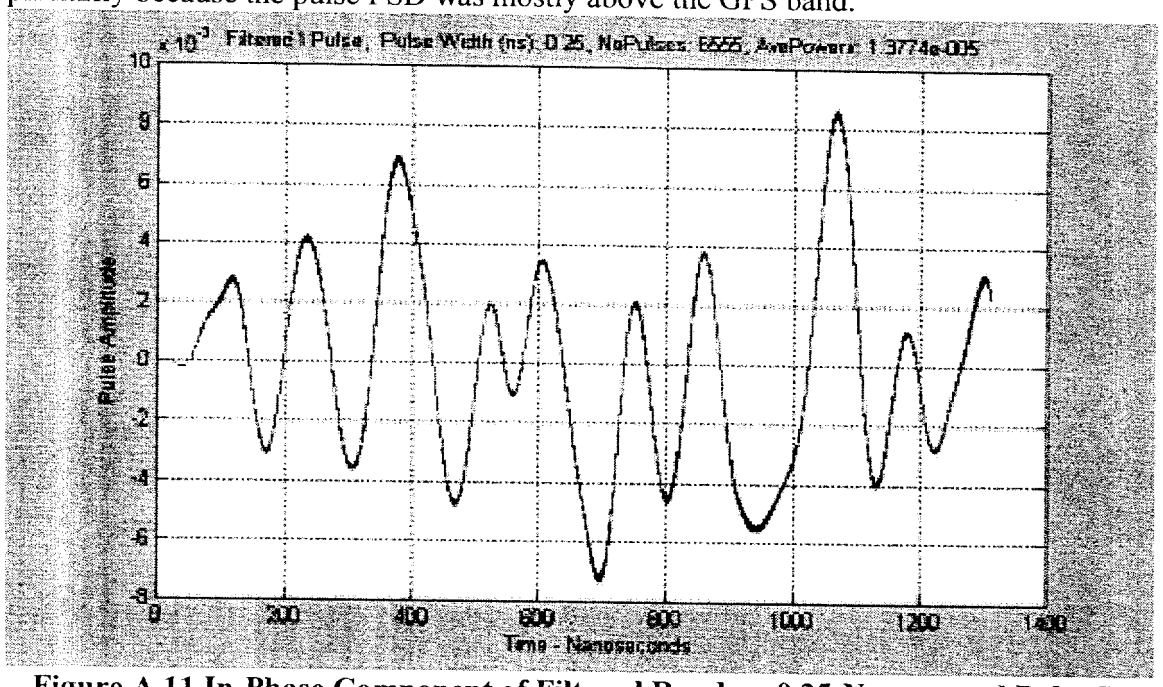

Figure A.11 In-Phase Component of Filtered Random 0.25-Nanosecond Pulse Sequence

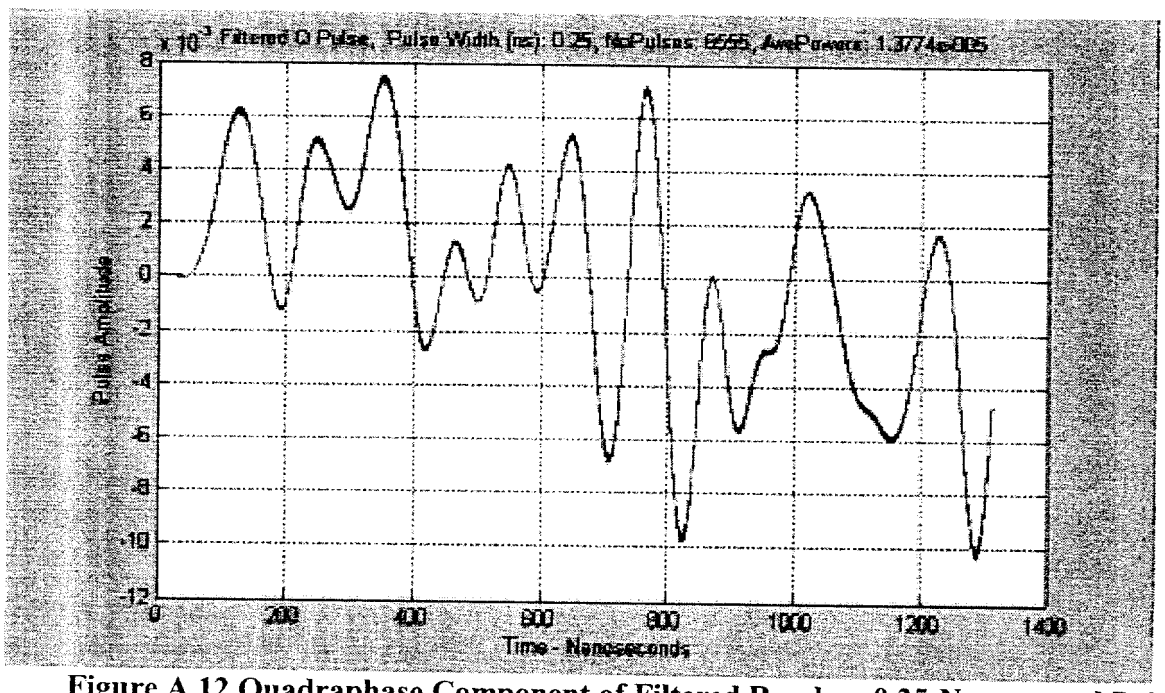

Figure A.12 Quadraphase Component of Filtered Random 0.25-Nanosecond Pulse Sequence

It is truly observable in Figures A.11 and A.12 is that the filtered output is essentially random with respect to the time-scale of the C/A code chips and subsequent correlation and smoothing in

the receiver (1 millisecond or more). Thus, the effect of random UWB pulses on a GPS receiver is truly that of wideband noise.

The filtered response to the one-nanosecond pulses is very similar, except that the power reduction is much less. This is because much of the unfiltered pulse power is in the GPS band.

The filtered response to the constant PRF sequence resembles CW interference. The filtered response at RF is illustrated in Figure A.13. Again the figure is interesting, but it does not convey much detail. As before, conversion to baseband provides a much clearer picture of the filtered response. The converted In-Phase and Quadraphase responses are shown in Figures A.14 and A.15. Note that these responses truly do represent CW interference. In fact, the PSDs of these responses are that of spectral lines as is shown in Figures A.16 and A.17. These spectral lines could very well interact with the spectral lines of the C/A code.

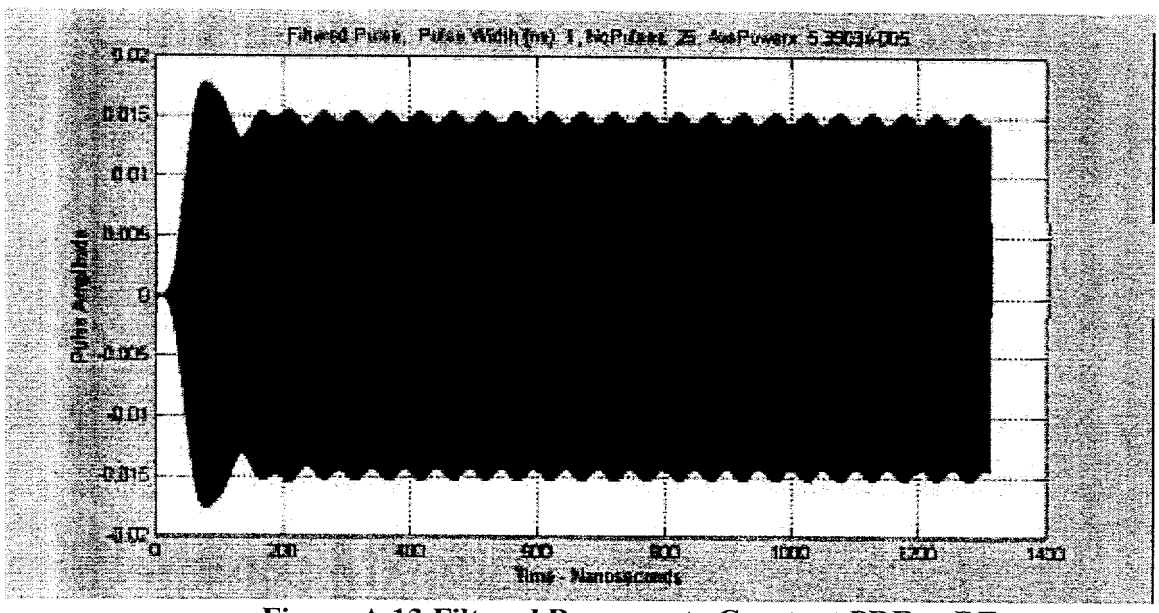

Figure A.13 Filtered Response to Constant PRF at RF

A.3 Pulse Collisions

As indicated above, the shape of the PSD of the transmitted pulses can change if pulses from different sources (or pulses due to multipath) collide and overlap in time. This is because the overlapping pulses correlate, or, in other words, generate a combined pulse that has a different shape. There is a mathematical basis for this that will be described here.

Consider two pulses that have identical shape, $x(t)$, except that one is delayed with respect to the other by Δt seconds, where Δt is less than the pulse width. The collision generates a new pulse $y(t)$, where

$$y(t) = ax(t) + bx(t + \Delta t) \qquad \text{A.1)}$$

where a and b represent different pulse attenuation. The autocorrelation function of the new pulse, in terms of the autocorrelation function of the original pulses, is then

$$\begin{aligned} R_y(\tau) &= \mathrm{E}\left[y(t)y(t+\tau)\right] \\ &= a^2\,\mathrm{E}\left[x(t)x(t+\tau)\right] + b^2\,\mathrm{E}\left[x(t+\Delta t)x(t+\Delta t+\tau)\right] \\ &\quad + ab\left\{\mathrm{E}\left[x(t)x(t+\Delta t+\tau)\right] + \mathrm{E}\left[x(t+\tau)x(t+\Delta t)\right]\right\} \\ &= \left(a^2+b^2\right)R_x(\tau) + ab\left[R_x(\tau+\Delta t) + R_x(\tau-\Delta t)\right] \end{aligned} \qquad \text{A.2)}$$

The PSD is defined as the Fourier Transform of the autocorrelation function, resulting in

$$S_y(\omega) = \left(a^2+b^2+2ab\cos\omega\Delta t\right)S_x(\omega) \qquad \text{A.3)}$$

The term in parenthesis reshapes the original PSD. To make this more clear, set $a = b = 1$. Then

$$S_y(\omega) = (2+2\cos\omega\Delta t)S_x(\omega) \qquad \text{A.4)}$$

If there is more than one pulse collision, the shaping coefficient simply becomes the some of the total number of pulse collision shaping coefficients.

Pulse collisions within the GPS receiver are much more probable because the filtering stretches the pulses and Δt can be much larger. Of course, this is accounted for in the graphs shown above. This is also true for the 19.6875 MHz PRF case, where the time between pulses is 50.8 nanoseconds. Due to filtering, the pulses are stretched much more than that. This is shown in Figure A.18 for one one-nanosecond UWB pulse. Thus, PSD shape within the receiver can change considerably and explains why the responses and PSDs in Figures A.14 through A.17 show a significant offset in frequency (about 5 MHz) when the input spectral line was right on the center of the filter.

A.4 Conclusions

From the responses shown above, it is very clear that the effect of UWB pulse sequences on a GPS receiver is much like random wideband noise, CW interference, and anything in-between, depending upon the pulse sequence (random, constant PRF or mixture of the two). Thus, the response to UWB emissions can be treated like any other GPS interference. That is, the random sequences can be treated like white noise and the constant PRF sequence can be treated like CW interference – treated as though it were 10 times worse than white noise. Any semi-random sequence would fit somewhere in-between. Thus, because the signal structure of UWB devices are unknown, the must be treated as the worst case CW interference at a 10 dB penalty with respect to white noise interference.

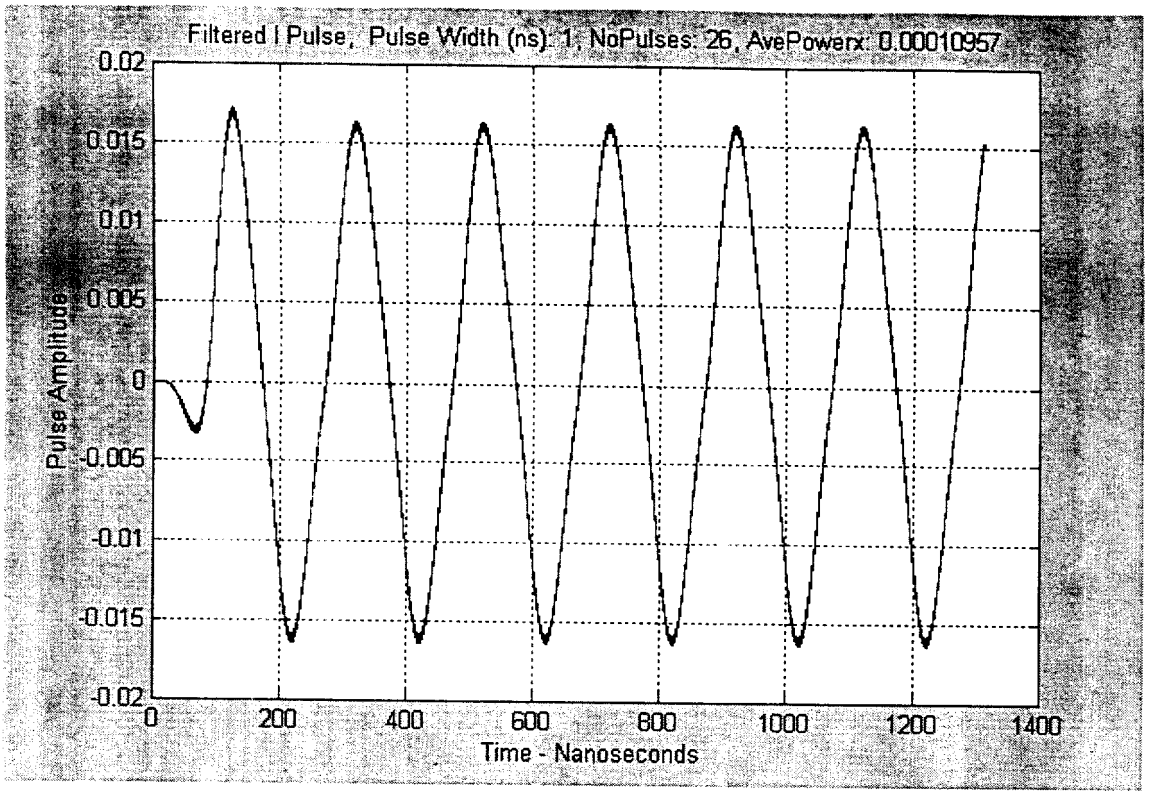

Figure A.14 Filtered In-Phase Response to Constant PRF Sequence

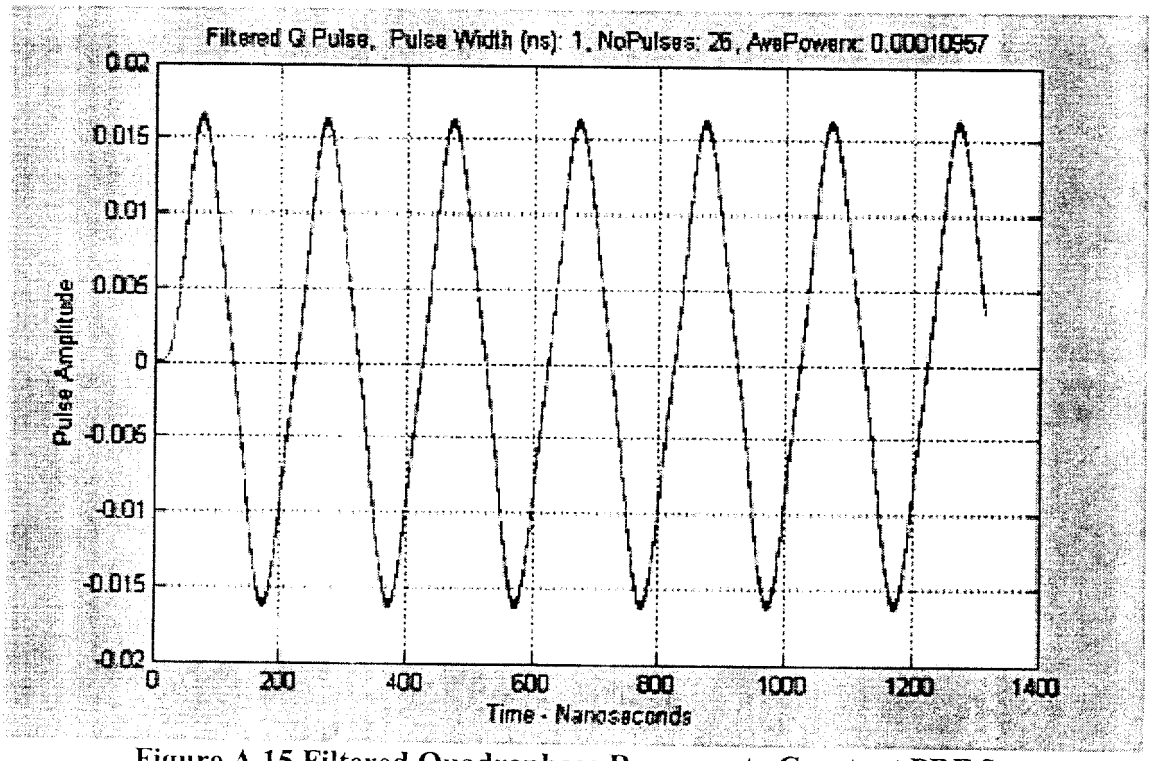

Figure A.15 Filtered Quadraphase Response to Constant PRF Sequence

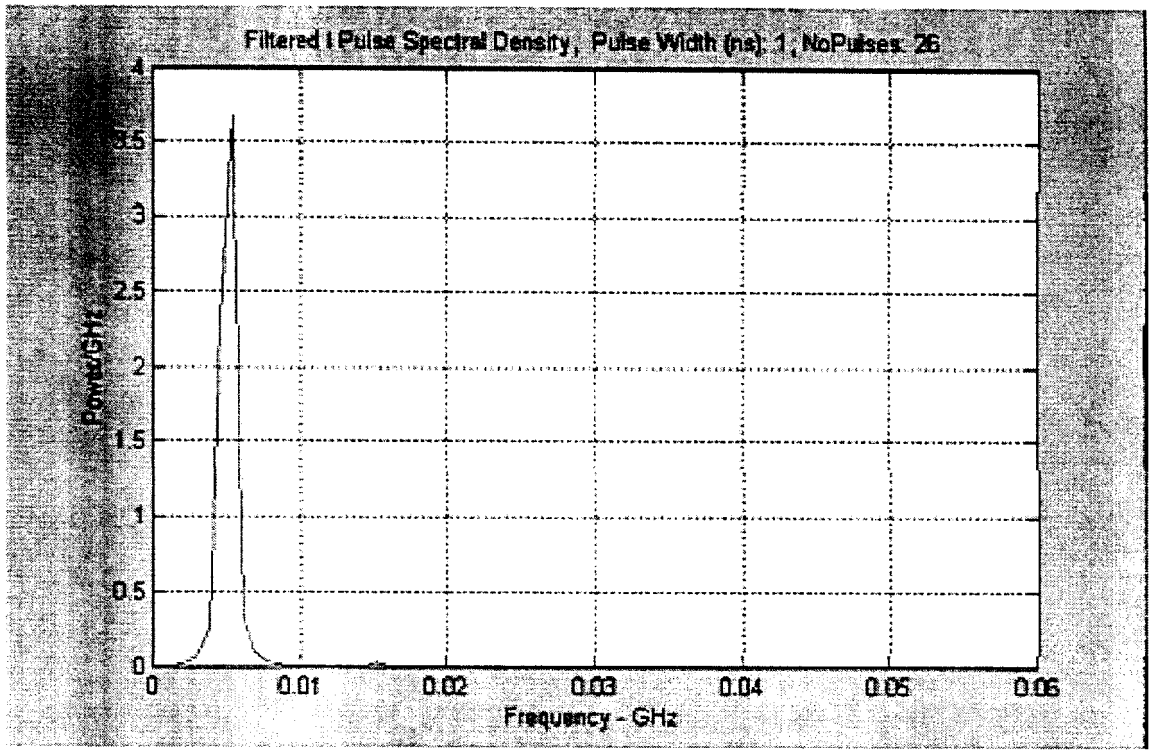

Figure A.16 PSD of Filtered In-Phase Component for Constant PRF Sequence

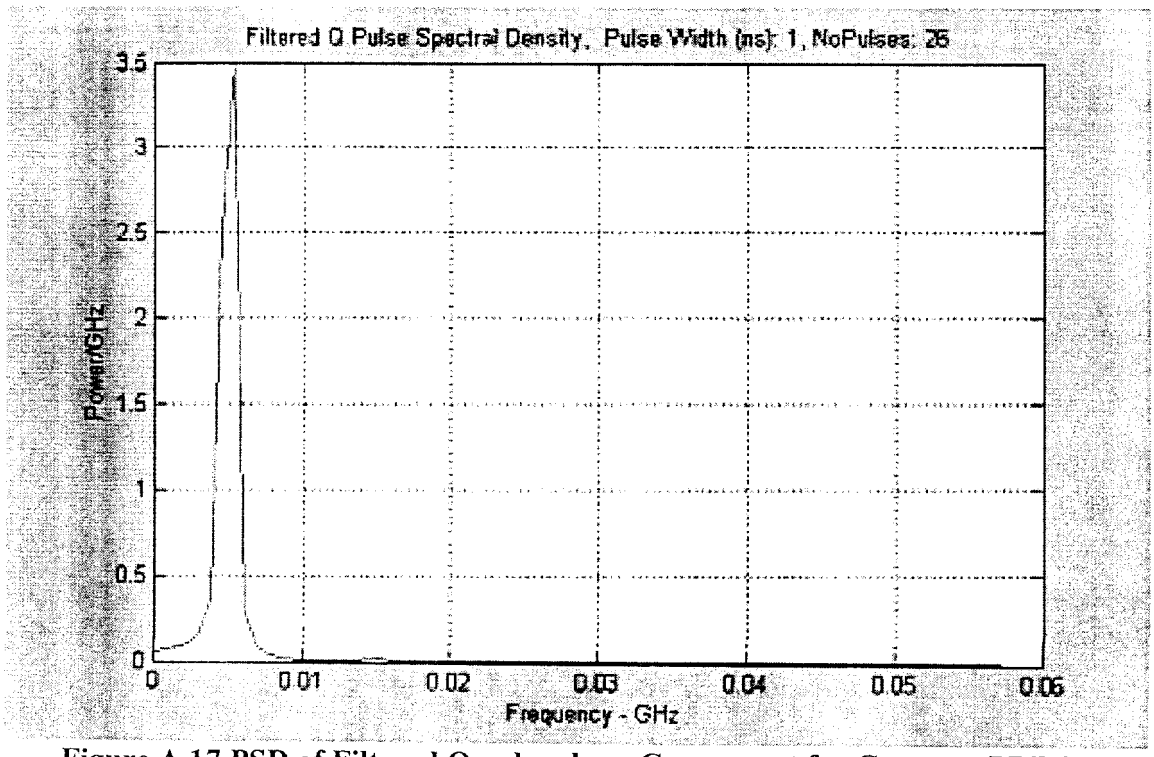

Figure A.17 PSD of Filtered Quadraphase Component for Constant PRF Sequence

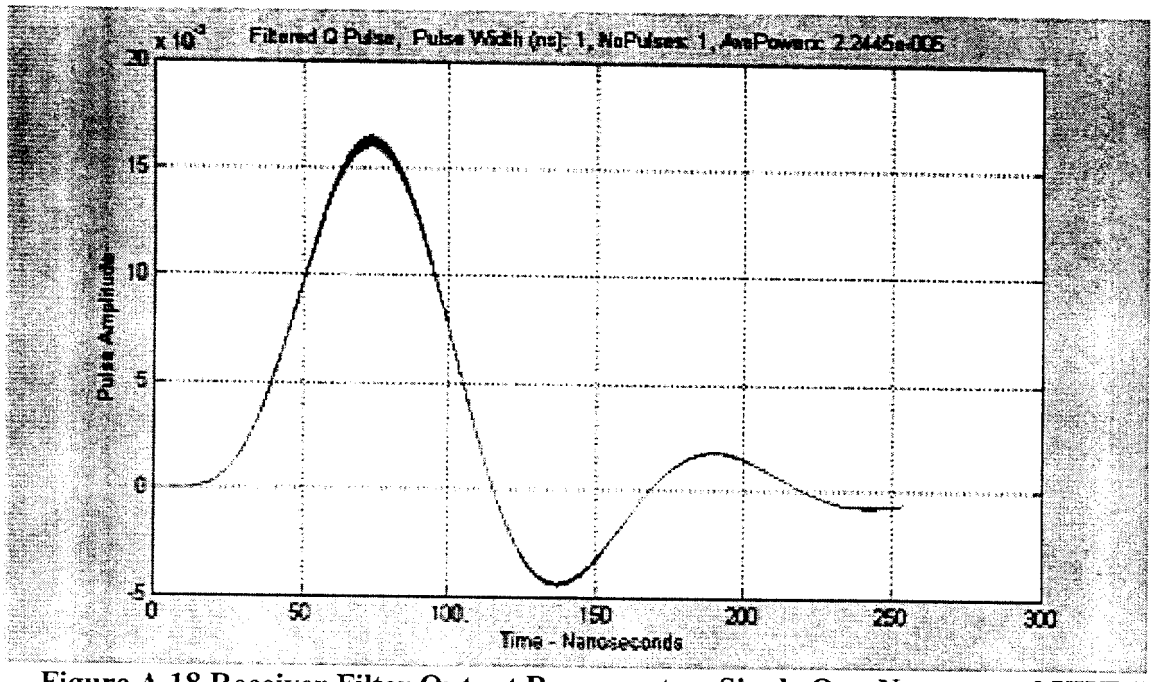

Figure A.18 Receiver Filter Output Response to a Single One-Nanosecond UWB Pulse

APPENDIX B GENERALIZED RFI EFFECTS COMPUTATION METHOD

The modulation formats of UWB transmissions can be characterized so that their RFI power can be simply estimated[33]. UWB signals are modeled as nanosecond and sub-nanosecond duration pulses that repeat with a pulse repetition frequency R_p. The victim receiver has bandwidth B_h whose center frequency is f_o. The effective duration of the receiver IF filter is ~ $1/B_h$. Each pulse has an energy spectral density, $\Phi(f_o)$. The output power of the filter due to input pulse sequence is P_{RFI}. There are 4 cases:

B.1 Case I: $B_{IF} < R_P$

Let R_P have constant intervals so that the Fourier transformation of the time sequence has a simple line spectra whose frequencies are multiples of R_P. The power in the spectral line $f_0 = jR_P$ is:

$$P_{RFI} = \Phi(jR_P)\, R_P^2. \qquad (1)$$

When $B_{IF} < R_P$, only one line component will lie in the pass band of the output filter. Thus the spectral lines are resolved and the output of the filter is a single line with power given by (1). In the time domain, the filter response time interval $1/R_h$ exceeds the pulse repetition time $1/R_P$. This is the worst case RFI modulation format for GPS receivers. Its broadband noise correction factor is –10 dB. Note: the RFI power increases as $20\log(R_P)$.

B.2 Case II: B_h << Average R_p

Let the pulse repetition rate be dithered (pulse position modulation) with average repetition rate of $\bar{R}_P$ and let $B_h << \bar{R}_P$. Then the output filter responses will overlap and the output time waveform will be a continuous random waveform whose probability distribution approaches Gaussian noise. UWB devices having this modulation format satisfied the broadband noise criteria and is the recommended RFI modulation format. Its broadband noise correction factor is zero. The output filter RFI power is:

$$P_{RFI} = \Phi(f_0) B_h \bar{R}_P \qquad (2)$$

Note: The RFI power increases as $10\log(\bar{R}_P)$.

B.3 Case III: B_h < Average R_p

Let the pulse repetition rate be dithered (pulse position modulation) with average repetition rate of $\bar{R}_P$ and let $B_h < \bar{R}_P$. There will be both continuous spectra and line spectra of varying strength at integer multiples of $\bar{R}_P$. The strongest lines will have power of:

---

[33] Pagett, J., "WINForum Response to FCC 98-208 NOI, Review of of Part 15 of the Commission's Rules Regarding Ultra-Wideband Transmission Systems," Attachment 1 'Analysis Ultra-Wideband Transmissions' Dec. 7, 1998

$$P_{RFI} = \Phi(f_0)\bar{R}_P^2 \qquad (3)$$

The position and intensities depend upon the pulse-position deviation relative to the average pulse rate deviation $1/\bar{R}_P$. Because of the presence of line spectra, Case III can have a broad band noise correction factor approaching –10 dB.

Note: The RFI power increases as $20\log(\bar{R}_P^2)$.

B.4 Case 4: $R_P << B_h$

When the filter bandwidth B_h is much greater than the pulse repetition frequency R_P, the pulses can be resolved in the time domain. In the frequency domain, the filter bandwidth spans many multiple spectral lines and cannot resolve them. This fact holds regardless of whether the pulse repetition frequency is dithered or not. This follows because the pulses are completely resolved in time. The filter output RFI power is:

$$P_{RFI} = \Phi(f_0)\, B_h^2 \qquad (4)$$

Note: The P_{RFI} varies as $20\log(B_h)$. Case 4 causes symbol interference in the victim receiver.

The four cases described above are the theoretical basis of the Stanford University and NTIA test results. In particular, they are the models that NTIA used to obtain their bandwidth correction factor methodology. Clearly these equations show why the UWB devices must be specified in terms of their modulation format. This is the reason why the broadband noise correction factor is necessary in the RFI link budget.

APPENDIX C LINE-OF-SIGHT PROPAGATION FROM MULTIPLE RFI SOURCES

An aircraft flying over ground-based RFI sources can have a relatively short line-of-sight distance and nearly equal path loss to a number of those sources. An RFI link budget factor that accounts for cumulative RFI effects from multiple RFI sources can be derived from consideration of the geometry below.

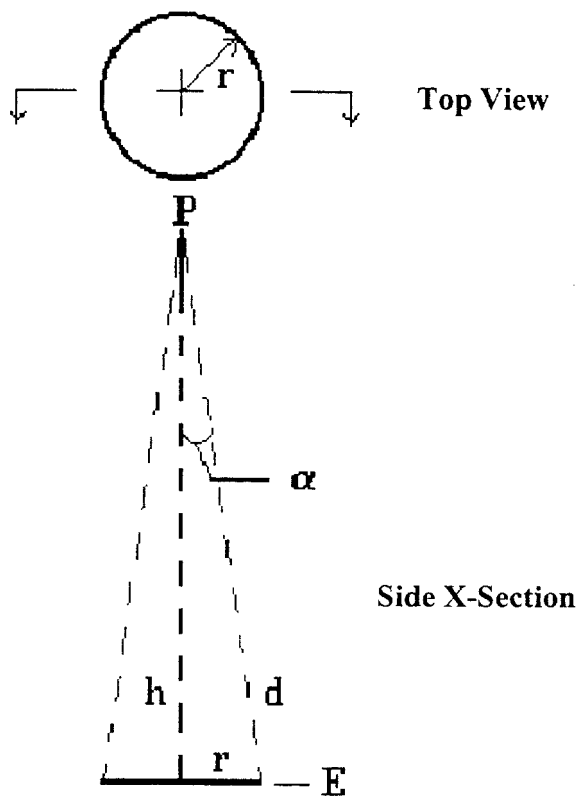

Figure C1. Geometry for Aircraft Overhead Pass of RFI Sources

In Figure C1, Point P represents the airborne GPS receive antenna and Surface E represents a planar surface containing RFI sources. Definitions for the geometric factors in the figure are:

h = minimum distance from P to plane E;

d = distance from points on E whose free-space propagation path spreading loss differs from the loss at distance h by a fixed ratio LR (loss is proportional to distance squared);

r = the radius of the circle containing the points of the fixed path loss ratio LR related to the length d; and

α = the angle between lines h and d, a GPS antenna pattern angle.

Since the propagation path spreading loss ratio between the paths of lengths d and h is given by

$$LR = d^2 / h^2 ,$$

and since the line segments *h*, *d*, and *r* form a right triangle so

$$r^2 = d^2 - h^2 ,$$

then simple substitution and algebraic manipulation yields the result:

$$\mathbf{r = h \bullet \sqrt{(LR - 1)}},$$

where $LR = \text{antilog}_{10}(LR_{dB} / 10)$.

The antenna pattern angle (α) is defined as $\cos^{-1}(h/d)$; thus

$$\boldsymbol{\alpha = \cos^{-1}(1/\sqrt{(LR)})}.$$

Use of the equations for circle radius, *r*, and antenna pattern angle, α, is illustrated by Category I aviation precision approach numerical examples where the closest antenna separation distance (*h*) is 100'. Consider loss ratio values (LR_{dB}) of 0.5, 1 and 3 dB. For the 0.5 dB ratio value:

$r = 100 \bullet \sqrt{(1.1220 - 1)} = 34.93$ feet (**69.9** feet diam.), and

$\alpha = \cos^{-1}(1/\sqrt{(1.1220)}) = 19.25$ degrees.

For a 1 dB loss ratio:

$r = 100 \bullet \sqrt{(1.2589 - 1)} = 50.9$ feet (**101.8** feet diam.), and

$\alpha = \cos^{-1}(1/\sqrt{(1.2589)}) = 26.97$ degrees.

For a 3 dB ratio:

$r = 100 \bullet \sqrt{(1.9953 - 1)} = 99.8$ feet (**199.5** feet diam.), and

$\alpha = \cos^{-1}(1/\sqrt{(1.9953)}) = 44.93$ degrees.

For the Category II precision approach minimum separation distance (h = 70'), the circle size for a given loss ratio scales down as *h* and antenna pattern angle remains constant.

These numerical examples illustrate several concepts. First, path loss increases rather slowly for fairly large horizontal separations from closest point below the airborne antenna. Second, antenna angles associated with small path loss ratios are small enough to neglect antenna gain variation. For larger path loss ratios, the antenna gain may actually increase for sources near the edge of the area and thus partially offset the effect on overall propagation path loss of the increased distance to those sources. Neglecting antenna gain variation is probably unwarranted for cases with larger than 3 dB loss ratio. Finally and most importantly, circular spaces around the closest RFI location associated with small path loss differences are large enough to contain several mobile sources. A common case where multiple sources might be visible is that of multiple vehicle-mounted UWB emitters in heavy traffic on a roadway below a runway approach.

APPENDIX D TOTAL SYSTEM ERROR STATISTICS

This appendix gives further analysis which justifies the minimum separation distance between a UWB emitter and an airplane performing a CAT II/III operation. Specifically, the statistical characteristics of the TSE are analyzed to show that the 21.9 ft of deviation below the glidepath assumed in the analysis in section 4.1.1 is reasonable.

D.1 Flight Technical Error

Requirements for flight technical error (FTE) in the vicinity of the category II decision height are defined in the FAA regulations for category II approval given in FAA AC 120-29A. These regulations require the airplane to be able to track the path to within +/- 35μA or +/-12 ft, whichever is larger. At 100 ft HAT, +/-12 ft is larger. AC 120-29A also recommends that excessive vertical deviation indications be implemented. On many modern airplanes, excessive vertical deviation indications are implemented such that some annunciation is given when the deviations exceed one half of full scale. At 100 ft HAT, this also corresponds to +/-12 ft. Even where special annunciation of excessive vertical deviations are not provided, it is common for standard operational procedures to specify that a go-around should be performed when the vertical deviations exceed 1 dot (on a 5 dot scale) or approximately one half full scale. This effectively creates a +/-12 ft window, which acts as a FTE probability distribution tail-cutter. Therefore, it is assumed pilots will maintain vertical course deviation within the Category II window which is half the full-scale deflection and where 0.7^{o} is full-scale deflection. The conversion from degrees to feet for ILS is given by the following equation: $[0.7^{o}\pi/180]$ $100/\mathrm{Tan}(3^{o}) = 23.3$ ft. The category II indicated window is ½ full scale or 23.3/2 = 11.65 ft ≈ 12ft. Typically, a pilot will do a go-around if he exceeds 1 dot deviation for a 5-dot display (2 dots above the glide path and 2 dots below the glide path). For an 11- dot display there would be 5 dots above the glide path and 5 dots below the glide path so the pilot would do a go-around if the deviation exceeds 2.5 dots.

The Advisory Circular requirements for a minimum system allow 5% of the approaches to exceed the +/-12 ft window. Thus a worst case FTE distribution would be represented by a normal distribution with a 1 sigma value of 6 ft. As a matter of practicality, the rate of missed approach is known to be much lower than 5%. Consequently, this analysis will also consider a nominal vertical FTE distribution such that 99.9% of the approaches remain within the +/- 12 ft window. This would result from a normal distribution with a 1 sigma value of 3.65 ft.

D.2 Navigation System Error

Navigation System Error (NSE) requirements for GBAS to support CAT II/III are not yet finalized and accepted internationally. Recent work indicates those previously proposed values for the Vertical Alert Limit (VAL) for CAT II/III may be unnecessarily stringent.[34] Nominal accuracy for GBAS is driven by the VAL. Typically, VPL_{H0} dominates and service is available if $VPL_{H0}<VAL$. Consequently, for the worst case geometry, the nominal 1 sigma vertical

[34] Murphy, T., et. al. "Considerations for GBAS to Support CAT II/III Operations", WP 19, ICAO GNSSP WG B, October 2000, Yokohama, Japan

accuracy is given by: VAL/K_{ffmd}. From the LAAS MASPS, for PT 2 & 3, VAL = 5.3 meters and K_{ffmd}=6.641. Using these values, the accuracy for the worst case acceptable geometry is 5.3/6.641 ≈0.8 meters 1 sigma.

There are 2 issues with using this requirement for the NSE.

1. The VAL requirement in the MASPS may be overly stringent. This could result in a significant penalty in service availability. Poor service availability could drive cost and complexity into the GBAS design (e.g. by requiring the addition of pseudolites to achieve useful levels of availability).

2. The use of the worst case geometry implicitly assumes that the continuity requirement (i.e. that the probability of a continuity event) is applicable to every single exposure interval and not representative of an average rate. Continuity requirements applied to every exposure interval are referred to as 'specific continuity' requirements, where continuity requirements that relate to an average rate are referred to as 'average continuity'. In some cases it is appropriate to use specific continuity rather than average continuity. In other cases, average continuity is the appropriate interpretation. For the case of CAT II/III operations, the choice between interpretation of continuity as specific continuity or average continuity is still somewhat controversial. A significant discussion on this topic by the international community will be required as a step in developing CAT II/III requirements for GBAS. Consequently we will examine the ramifications of both interpretations.

D.3 Accuracy of Worst Case Geometry vs. Accuracy Averaged Over all Geometries.

The instantaneous vertical accuracy depends on the satellite geometry, which varies as a function of time. Therefore the true distribution of errors when observed over a long period of time will be different than the distribution of errors for a specific worst case geometry. This is important because the worst case geometry should by definition be relatively rare for a system with good availability. In other words, the vast majority of the time the system will be operating much better than would be predicted by looking only at the worst case geometry that meets the VAL requirement.

Figure D1 illustrates the vertical error distribution averaged over time as it compares to the assumed distribution for the worst case geometry. We assume that for each geometry, the error is normally distributed with a 1-sigma variation equal to the VPL/6.641. An availability analysis was run to look at the probability distribution of the values of VPL over all time. This was done by computing the satellite geometry at 1 minute intervals using the Martinez constellation, and accounting for up to 4 satellite failures. This pdf of the VPL is then used to develop a weighted sum of normal distributions which represents the time averaged vertical error distribution.

From the figure it can be seen that the distribution of vertical error averaged over all time and constellation states is significantly tighter than the normal distribution corresponding to the worst satellite geometry that would meet a VAL of 10 meters. The circles on the plots show the 'equivalent 5-sigma points" or the points for which the integration of the tails gives a probability mass equal to the mass in the tails of a Gaussian distribution outside 5 sigma.

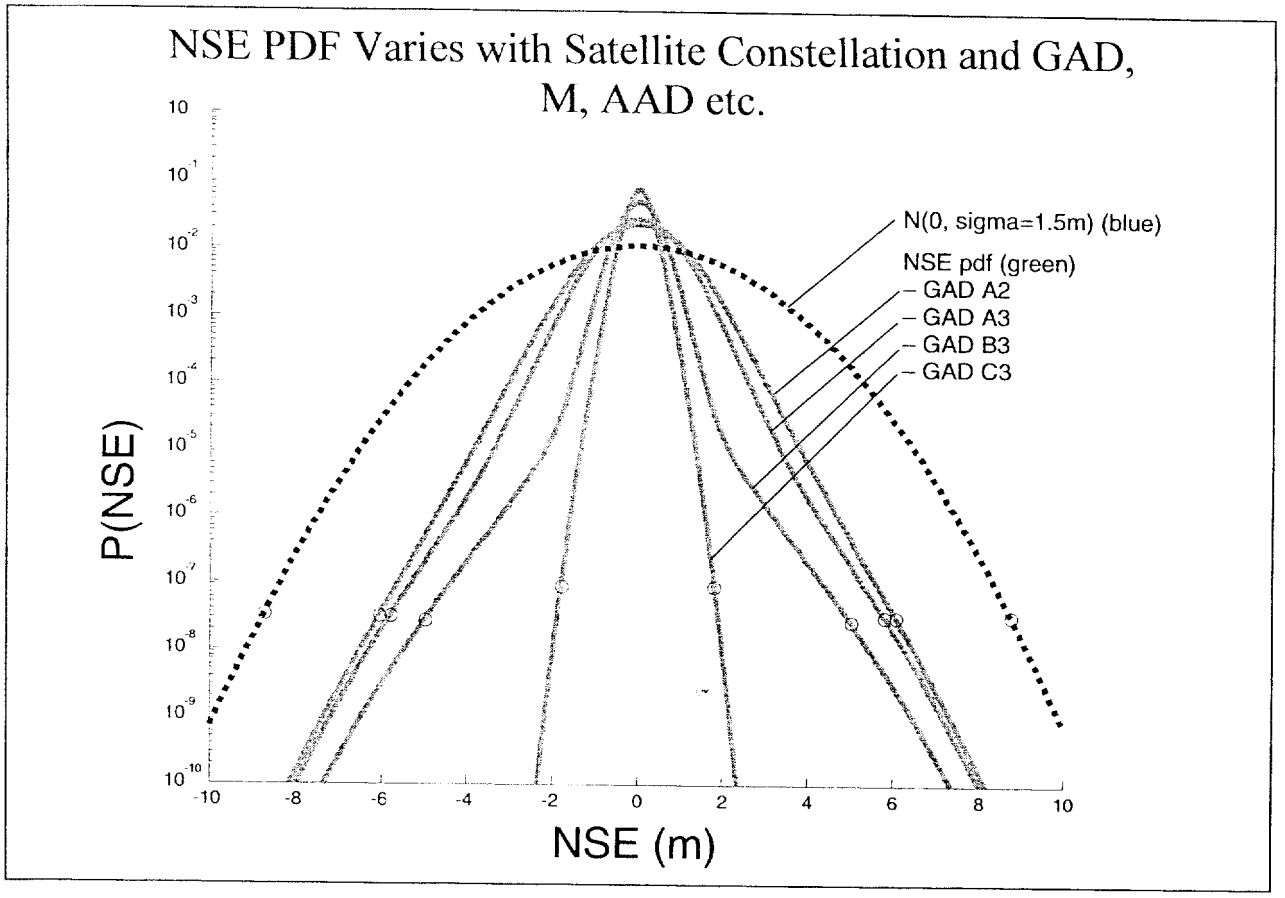

Figure D1 GBAS NSE Distribution Averaged over All Geometries that Meet VAL<10 Meters

D.4 Total System Error Calculation

The TSE distribution is based upon the FTE and NSE distributions. FTE and NSE add, so the distribution of TSE can be obtained by convolving the distributions for FTE and NSE. Five cases were considered. The assumed distributions for each of the cases are listed in Table D1. Two different Gaussian distributions were assumed for FTE: one with σ_{FTE} =6 ft and the other with σ_{FTE} =3.65ft. Both distributions were truncated to +/-12 ft. The cases with σ_{FTE} =6 ft correspond to performance that just meets the required tracking accuracy (i.e. +/-12 ft 95%). The cases with σ_{FTE} =3.65 ft represent tracking accuracy which is better than the requirement and results in 99.9% of the approaches remaining within the +/-12ft window. This is believed to be a more realistic case as the rate of go-arounds is clearly less than 1 in 20 approaches as would be implied by performance that just meets the 95% requirements (assuming the pilot would typically do a go around when FTE exceeds one half full scale).
Three different cases for NSE are considered:

1. Vertical NSE Gaussian distribution with σ_{vert} =0.8 meters. This corresponds to the case where VAL = 5.3 meters.
2. Vertical NSE Gaussian distribution with σ_{vert} =1.5 meters. This corresponds to the case where VAL = 10 meters (and VPL is computed using the K factors appropriate for PT 2).

3. Vertical NSE as observed over all time and satellite constellation states (appropriately weighted by the probability of being in each particular state). For this case, the vertical NSE pdf will depend on the characteristics of the GBAS ground station and airborne equipment (i.e. Ground Accuracy Designator (GAD), Airborne Accuracy Designator (AAD), and number of reference receivers in the GBAS ground station). We assume in all cases that the performance of the ground station is characterized by GAD B3, and the airborne is characterized by AAD B. (It is unlikely that GAD A ground stations will provide useful availability for PT 2 service and that 3 reference receivers will be needed to meet the overall continuity requirements. Consequently, GAD B3 is representative of the worst case ground facility to support CAT II operations). (Figure D1)

Table D1 Assumed FTE and NSE Distributions for the Five Cases Considered

Case	Assumed FTE Distribution	Assumed NSE Distribution	Comments
A	N(0 , σ_{FTE}=6 ft) Truncated at +/- 12 ft	N(0, 0.8 m) Truncated at 5 $\sum$	Baseline assumptions
B	N(0 , σ_{FTE}=6 ft) Truncated at +/- 12 ft	N(0, 1.5 m) Truncated at 5 $\sum$	Baseline assumptions except NSE consistent with VAL of 10 m for PT 2 .
C	N(0 , σ_{FTE}=3.65 ft) Truncated at +/- 12 ft	N(0, 1.5 m) Truncated at 5 $\sum$	FTE such that 99.9% of approaches remain within +/- 12 ft window. NSE consistent with VAL of 10 m for PT 2.
D	N(0 , σ_{FTE}=6 ft) Truncated at +/- 12 ft	Vertical Error pdf averaged over time and satellite constellations. No truncation	FTE such that 95% of approaches remain within +/- 12 ft window. Time averaged NSE with GAD B3 and AAD B.
E	N(0 , σ_{FTE}=3.65 ft) Truncated at +/- 12 ft	Vertical Error pdf averaged over time and satellite constellations. No truncation	FTE such that 99.9% of approaches remain within +/- 12 ft window. Time averaged NSE with GAD B3 and AAD B.

For each case in Table D1 the convolution of the assumed FTE and NSE distributions was computed. Figure D2 illustrates the assumed distributions and the result of the convolution of the distributions for Case E in Table D1. The TSE distribution function corresponding to the random variables FTE and NSE will not be Gaussian. Next, the probability that the magnitude of the TSE exceeds x was computed based on the following relationship:

$$p(|TSE| > x) = 1 - \int_{-x}^{x} pdf_{TSE}(y)dy$$

where:

$pdf_{TSE}(y)$ - is the result of the convolution of the FTE and NSE distributions.

For RFI considerations of ground-based mobile emitters we are only interested in the deviations below the glide path.

Figure D3 shows a plot of the probability that TSE exceeds an arbitrary number of feet for the 5 cases listed in Table D1. The point of interest is where each curve crosses 21.9 ft. Case A (based on the assumptions in earlier work) results in a very low probability that TSE exceeds 21.9 ft below the flight path[35]. Increasing the NSE to correspond to a VAL of 10 meters (case B), results in a significantly higher probability that TSE will exceed 21.9ft (i.e. on the order of $2x10^{-3}$).

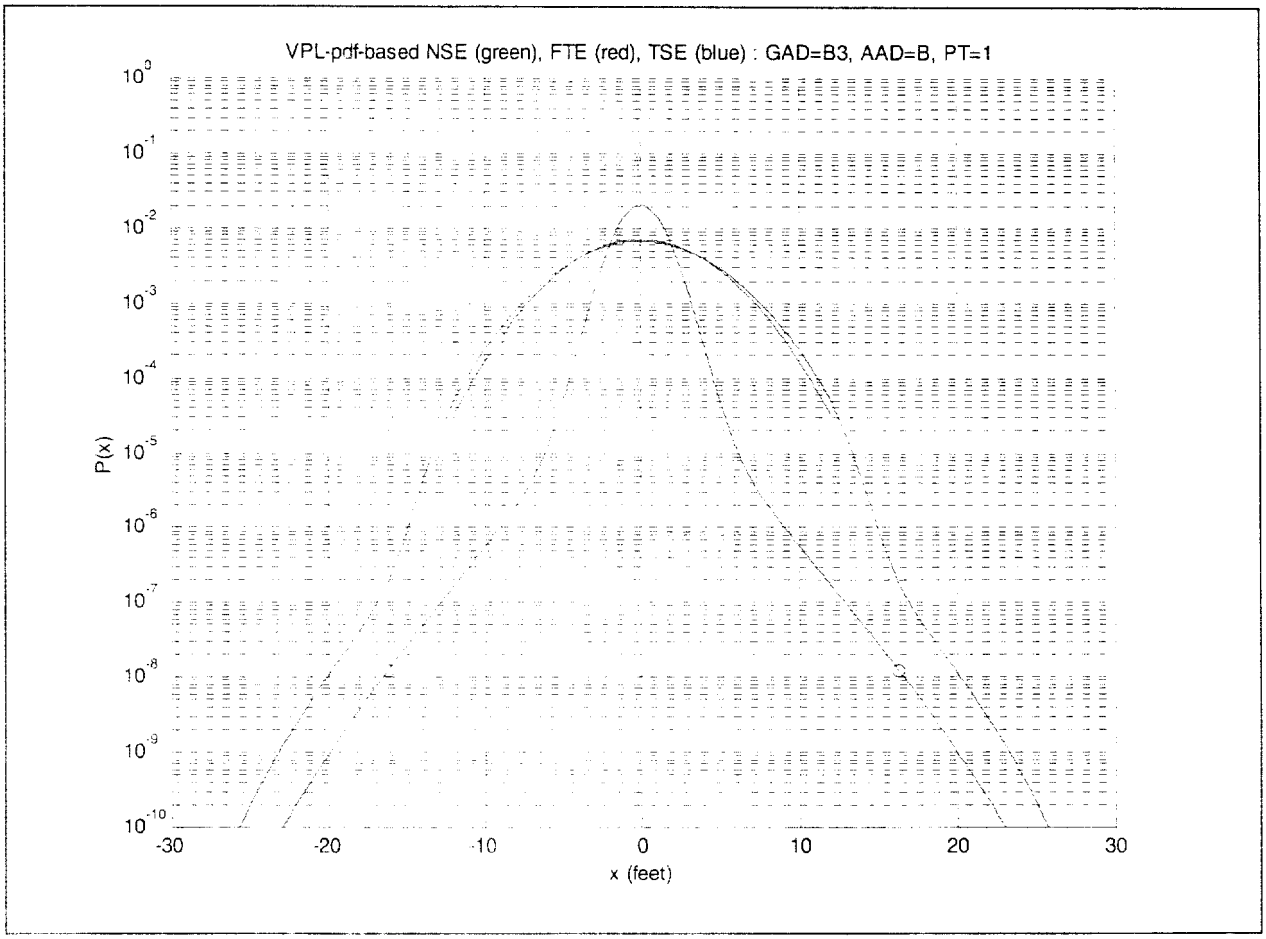

Figure D2 Convolution of Assumed FTE and NSE distribution

Assuming a lower variance of FTE (Case C) improves the situation somewhat, but the probability that TSE exceeds 21.9 ft is still high (i.e. on the order of $4x10^{-4}$). If the time average NSE distribution is used with the more pessimistic FTE assumptions (Case D), the probability that TSE exceeds 21.9 ft is again appropriately low ($\approx 3x10^{-6}$). Using the average NSE in conjunction with the more realistic FTE, (Case E), the probability that TSE exceeds 21.9 ft is even smaller than the baseline case described in earlier work ($\approx 7x10^{-7}$).

[35] The analysis in earlier work apparently did not use integration of a single tail. Consequently the probability values ($2.87x10^{-7}$) are lower than those computed in this analysis given the same assumptions ($\approx 2x10^{-6}$).

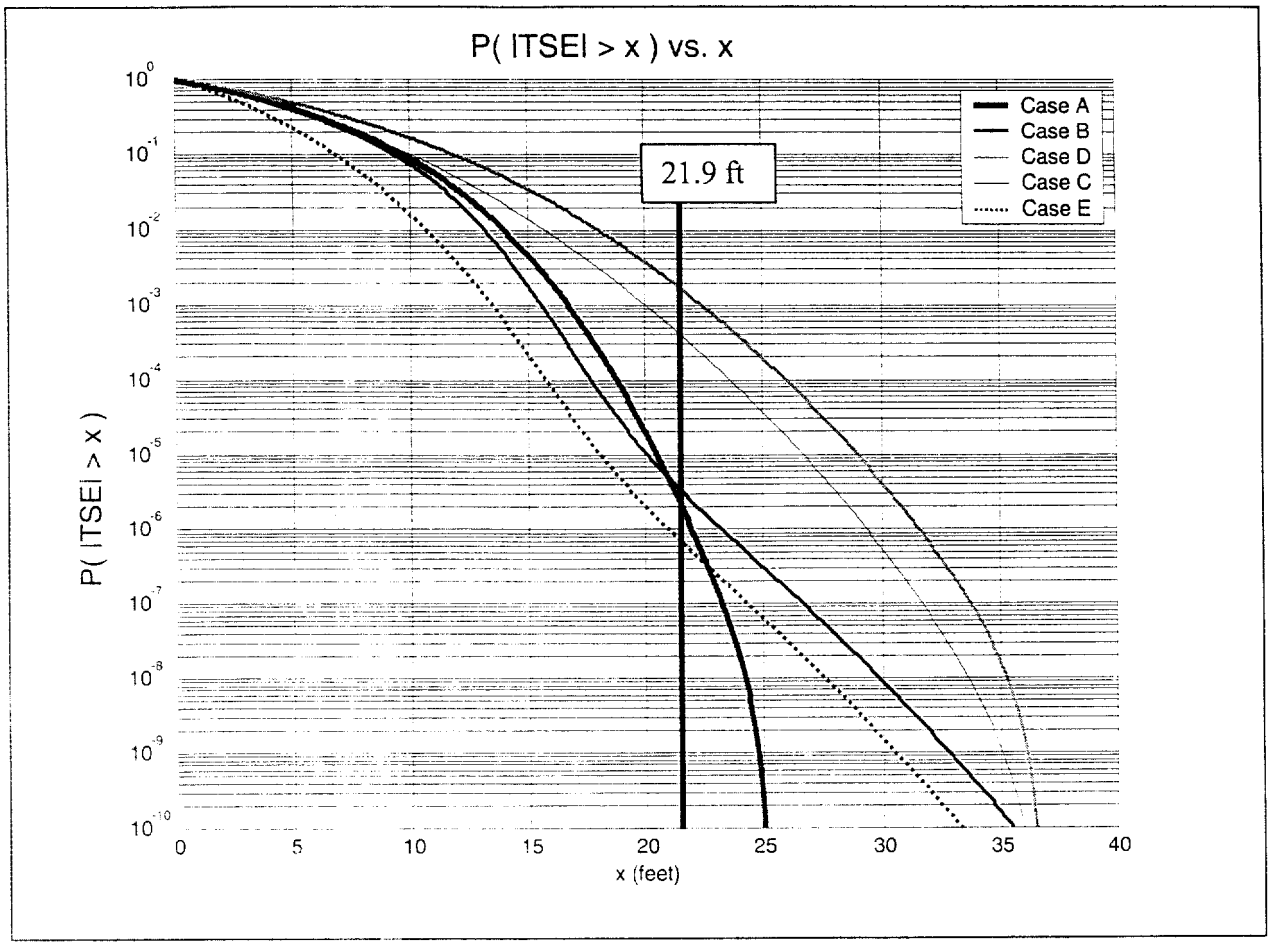

Figure D3 Probability that |TSE| > X Given the Assumed Distributions of FTE and NSE.

D.5 Summary and Recommendations

Examination of Figure D3 shows that the probability that TSE exceeds 21.9 ft, given the assumed distributions of NSE and FTE, is appropriately low for Cases A, D and E. As Case A is based on worst case, specific continuity risk (rather than average continuity) and the assumed NSE is possibly smaller than what is required.

Use of average continuity risk rather than (specific continuity risk) results in probabilities that the minimum separation distance is exceeded on the order of 10^{-6}. This seems like a very reasonable allocation for the continuity risk for this RFI event. The single-sided LAAS system continuity is $2x10^{-6}$ per 15s. Both of these contributors are arguably insignificant when compared to the probability of a go-around due to FTE alone ($1x10^{-3}$ to $5x10^{-2}$ according to the assumptions used in this analysis)